This is to certify that the

thesis entitled

EFFECT OF HYPERCAPNIA
ON CEREBROSPINAL FLUID (CSF) DYNAMICS

presented by

Warren Dang

has been accepted towards fulfillment
of the requirements for

___M.S.___ degree in __Physiology__

_____
Major professor

Date__August 28, 1980__

O-7639

EFFECT OF HYPERCAPNIA

ON CEREBROSPINAL FLUID (CSF) DYNAMICS

By

Warren Dang

A THESIS

Submitted to
Michigan State University
in partial fulfillment of the requirements
for the degree of

MASTER OF SCIENCE

Department of Physiology

1980

ABSTRACT

EFFECT OF HYPERCAPNIA ON

CEREBROSPINAL FLUID (CSF) DYNAMICS

By

Warren Dang

The brain ventricles of anesthetized cats were
perfused with an artificial CSF containing sucrose and inulin
while the animals inspired room air and 8-10% CO_2-in-air gas
mixture (hypercapnia). Steady state measurements of
perfusion inflow and outflow rates and test molecule
concentrations (C_o's) allowed for calculations of CSF
formation ($\dot{V}_f$) and absorption ($\dot{V}_a$) rates and a permeability
coefficient for sucrose (K_{suc}). CSF perfusion volumes (V_D)
were determined by integrating C_o's as a function of time.
Hypercapnia caused increases in $\dot{V}_f$, K_{suc} and perfusion
effluent ($\dot{V}_o$) while $\dot{V}_a$ and V_D remained unchanged.
Hypercapnia induction caused transient increases in $\dot{V}_o$ and
intraventricular pressure and a transient decrease in C_o's
and were to a large extent reversible upon hypercapnic
withdrawal. These results suggest that $\dot{V}_f$ and K_{suc} are blood
flow dependent and that hypercapnia increases brain blood
flow and brain blood volume causing a competitive
displacement of CSF volume.

ACKNOWLEDGEMENTS

Many people have contributed significantly throughout the course of this study, and the author wishes to express his sincere graditude to all.

The author wishes to thank his mentors, Drs. S. R. Heisey and T. Adams, for their constructive and valuable criticism, and moral encouragement throughout this program and to the third member of his guidance committee, Dr. L. F. Wolterink, for his valuable assistance on the preparation of this thesis.

TABLE OF CONTENTS

Page

LIST OF TABLES

LIST OF FIGURES

I. INTRODUCTION

Cerebrospinal fluid (CSF) in vertebrates fills the cerebral ventricles, and the subarachnoid space surrounding the brain and spinal cord. CSF is a clear, colorless fluid which flows from the two lateral cerebral ventricles through the foramina of Monro into the third ventricle, then through a narrow channel, the aqueduct of Sylvius, into the fourth ventricle. The foramina of Magendie and Luschka connect the fourth ventricle with the subarachnoid space surrounding the brain and spinal cord.

The composition of CSF is actively regulated at various sites in the brain, among which are the choroid plexuses which project into the ventricles. These are highly vascularized modifications of the pia mater which lie in the lateral, third and fourth ventricles. The blood flow through the choroid plexus, as measured in the rabbit, is 3 ml/min per gram of choroid plexus tissue, and the total choroidal production of CSF is 25% of this rate (Welch, 1963). CSF is formed also by extrachoroidal tissue (Milhorat et al., 1971) and Pollay and Curl (1967) have suggested that 31% of total CSF formation may originate from these sources.

1

CSF, produced in the ventricular system, is reabsorbed back into blood in the cerebral venous sinuses. The arachnoid membrane surrounding the subarachnoid space contains micro-and macroscopic villus-like projections into the venous sinuses (Weed, 1914). The structure of these villi is such that they act as one-way valves permitting flow of CSF as well as particles up to 7 microns in diameter into the blood when CSF pressure is approximately 10 mm H_2O greater than the venous sinus pressure (Welch and Friedman, 1960).

Substances injected into the peripheral blood circulation are restricted from passively entering the brain and CSF. Vital dyes such as trypan blue when injected intravenously, stain most body tissues while the brain remains relatively unstained (Tschirgi, 1950). The restricted dye movement from the blood into brain tissue and CSF has led to the concept of blood-brain and blood-CSF barriers. These postulated barriers restrict free diffusion along concentration gradients for many large molecules, notably plasma proteins (albumin) into the brain and CSF. Even ions such as potassium and calcium are actively maintained at constant concentrations in the CSF and brain despite variations in their plasma concentration (Katzman et al., 1965; Graziani, 1967).

There is a great deal of information concerning the anatomy and physiology of the cerebrospinal fluid, CSF formation and absorption rates and the transependymal

exchange of substances between CSF and brain and CSF and blood. Many studies which have provided this information have been specifically designed for conditions in which the cerebral hemodynamics, brain blood flow and brain vascular volume have been assumed to be normal and stable.

Hypercapnia produces an increase in brain blood flow (Wolff and Lennox, 1930; Kety and Schmidt, 1948; Reivich, 1964) which causes an increase in intracranial blood volume (Smith et al., 1971; Grubb et al., 1974). In rabbits and guinea pigs, during normocapnia, intravenously injected trypan blue does not enter the brain parenchyma, but during hypercapnia the brain is stained by this dye (Clemedson et al., 1958). Others have shown in dogs and cats that intravenously administered I-125 albumin penetrates into CSF and brain more readily during hypercapnia than during normocapnia (Lending et al., 1961; Hochwald et al., 1973).

Studies of the effect of hypercapnia on CSF formation and absorption rates are inconclusive. Hochwald et al. (1973) demonstrated that there is as much as a 50% reduction in the absorption rate of CSF during hypercapnia while CSF formation either increased above normocapnic rates (Ames et al., 1965), or did not significantly change during hypercapnia (Hochwald et al., 1973; Martins et al., 1976).

The aim of the present study was to evaluate the influence of 8-10% CO_2 inhalation on CSF dynamics using the ventriculocisternal perfusion technique (Pappenheimer et al., 1962) to measure CSF formation and absorption rates,

transependymal exchange rates, and to evaluate changes in
intracranial CSF volume using compartmental analysis techniques.

II. LITERATURE REVIEW

2.1. Cerebrospinal Fluid Production

2.1.1. Cerebrospinal fluid production by the choroid plexus

The choroid plexuses have long been implicated as a major site of cerebrospinal fluid (CSF) production. Some of the first studies which demonstrated that production of CSF occurred within the cerebral ventricular system were conducted by Dandy and Blackfan (1914) and Frazier and Peet (1914). They experimentally produced bilateral hydrocephalus by blocking the aqueduct of Sylvius with cotton pledgets, and observed abnormal ventricular distention proximal to the blockage, indicating that CSF is formed within the cerebral ventricles. Dandy (1919) later showed that the source of CSF production in the cerebral ventricles was the choroid plexus. He removed the choroid plexus from one lateral ventricle of the dog while blocking both foramina of Monro. This resulted in the development of a unilateral hydrocephalus in the non-plexectomized ventricle.

De Rougemont et al. (1960) provided direct

experimental evidence that the choroid plexus produces CSF. They developed a technique for collecting, _in situ_, fluid secreted directly by the choroid plexus in cats. The lateral ventricle was surgically exposed and the CSF was replaced with a dense oil. Since choroidal tissue is lighter than the oil, it rose from the ventricular walls and fluid formed on its upper surface. A glass pipette was lowered through the oil and samples of fluid were collected over a 2 to 10 minute period. Since the composition of the collected fluid was similar to the CSF collected from the cisterna magna, the authors concluded that the choroid plexus is a source of CSF production.

Welch (1963) devised a method for estimating CSF production by the rabbit choroid plexus. He cannulated the large choroidal vein which drains most of the blood from a lateral ventricular plexus and measured its linear flow velocity from motion pictures of the movement of an 1-octanol bubble injected into the choroidal vein. Total choroidal blood flow was estimated by calculations which related linear blood flow to the radius of the vessel, the proportion of the plexus drained by the main choroidal vein, and choroid plexus weight. He estimated choroidal blood flow to be 2.86 μl/min per mg of plexus tissue. Plasma volume loss during the passage of blood through the plexus was calculated from the difference between arterial and choroidal venous hematocrits. CSF secretion was estimated from the choroid plexus blood flow and the fractional plasma volume loss during the transit

of blood through the plexus. A CSF production rate of 0.37 μl/min per mg of choroidal tissue was calculated. From this and the weight of all choroid plexus tissue, he calculated total choroidal CSF production to be 7.8 μl/min.

2.1.2. CSF production by extrachoroidal sources

Although experimental evidence favors the hypothesis that the choroid plexus tissues are the main secretory sites of CSF formation, the ventricular ependyma also has been implicated as its source (Pollay and Curl, 1967). These investigators perfused the aqueduct of Sylvius and the anterior fourth ventricle in the rabbit, an area which does not have choroid plexus tissues. They found a mean rate of CSF formation of 0.33 μl/min per cm^2 of ependymal surface using an inulin dilution principle (Heisey et al., 1962). The perfused area of the rabbit's ventricular ependyma, estimated by photographic planimetry was 12.8 cm^2. This lead them to predict a CSF formation for the ventricular ependyma of 4.23 μl/min. Since the total CSF production in the rabbit was 12.67 μl/min they concluded that approximately 31% of CSF produced could be attributed to the ventricular ependyma. Milhorat et al. (1971) observed that CSF production rate in the bilateral plexectomized rhesus monkey (13.3 μl/min) was reduced by only 31%, compared to normal monkeys (19.9 μl/min). They also reported that CSF composition after choroid plexectomy remained relatively unchanged during ventriculo-aqueductal perfusion to a blocked aqueduct of

Sylvius. In an earlier study, Milhorat (1969) reported that in monkeys, the choroid plexus may not be the major source of CSF production. They suggested that it is either a secretion of the ventricular ependyma or a fluid that is produced by cerebral metabolism which enters the ventricle across the ependymal lining.

2.1.3. Quantitative measurement of CSF production

Quantitative measurement of CSF production, in vivo, was made by Flexner and Winters (1932) using anesthetized cats. A cannula with an inflatable cuff was placed in the posterior portion of the aqueduct of Sylvius and the cuff was inflated to provide a seal around the cannula. The amount of fluid (CSF) flowing from the aqueduct was collected and its volume measured using a bubble-manometer. This is a volume displacement device consisting of a scale which converts the distance traveled by an air bubble in a column of oil solution into a volume permitting the estimation of the rate of CSF produced. A fluid reservoir was attached to one end of the manometer so that the intraventricular pressure remained constant. At a ventricular pressure of 110 $\pm$ 10 mm H_2O, approximately, 8.4 μl/min or 12 ml/day of fluid was collected which represented CSF formed by the lateral and third ventricles. They assumed that the amount of CSF produced by a single choroid plexus is directly proportional to it weight, and that the choroid plexus of the fourth ventricle weighed about 25% of the total weight of all

plexuses. They estimated that the fourth ventricle would contribute approximately 2.1 µl/min yielding a total CSF formation rate of 10.5 µl/min.

Bering (1959) measured CSF production by a passive drainage technique. A cannula was inserted into the cisterna magna of anesthetized dogs and the amount of CSF was measured using a bubble-manometer (as described by Flexner and Winters in 1932) to estimate CSF formation rate. The end of the cannula was 50 mm below the level of the right heart in order to produce a maximum outflow of CSF and to prevent CSF absorption in the subarachnoid space. Bering reported that the collected fluid had the same composition as CSF secreted from choroid plexus tissue and estimated a CSF formation rate of 50 µl/min.

2.1.3.1. Ventriculocisternal perfusion

There is an improvement in the quantitative measurement of CSF production if a ventriculocisternal perfusion technique is used (Pappenheimer et al., 1962). With this technique, cannulae are implanted in the lateral ventricle and cisterna magna, and an artificial CSF is perfused into one lateral ventricle and outflow is collected from the cisterna magna. The presssure in the CSF system is set by the height of the outflow tubing relative to the auditory meatus which is defined as zero hydrostatic pressure. Inflow and outflow volume flow rates and steady-state concentrations of test substances are measured

so that molecular clearances in the perfused CSF system can be calculated. By adding a large, non-metabolizable molecule such as inulin (M.W.= 5200) to the perfusion inflow they estimated CSF formation as well as a bulk fluid absorption rate in the ventriculocisternal system. They found that inulin does not diffuse across the ventricular ependyma, since at intraventricular pressures of -15 cm H_2O, all inulin entering the lateral ventricle was recovered in the cisternal outflow (Heisey et al., 1962). Therefore, any dilution of inulin during its passage through the cerebral ventricles to the cisterna magna is assumed to result from newly-formed, inulin-free fluid secreted by the animal. This method has been used in a variety of vertebrate species with other high molecular weight substances (Table 1).

2.1.4. Factors affecting CSF formation

The effects of drugs on CSF formation yields important information about the mechanisms of CSF secretion. For example, Pollay and Davson (1963) reported that in rabbits CSF formation is reduced by 50% after the intravenous or intracisternal administration of acetazolamide (Diamox). Similarly, Welch (1963) observed an 85% reduction in CSF formation whether Diamox was administered intravenously or by topical administration to the isolated choroid plexus. Maren (1967) proposed that carbonic anhydrase inhibitors decrease the metabolic formation and dissociation of carbonic acid (H_2CO_3) which may be a necessary link in the chemical

Table 1. Species variation in cerebrospinal fluid formation rate ($\dot{V}_f$) and Resistance to CSF absorption

SPECIES	$\dot{V}_f$	Resistance to CSF Absorption	Reference Molecules	Investigators
	($\mu l/min$)	($cm\ H_2O/\mu l \cdot min^{-1}$)		
Turtle	1.4	1790	I-131 Albumin	Heisey and Michael (1971)
Chicken	1.4	4545	I-131 Albumin	Anderson and Heisey (1972)
Rat	2.2	-	Inulin	Cserr (1967)
Rabbit	13.0	169	Inulin, ^{3}H-Inulin	Pollay and Curl (1967)
Cat	21.0	390	Inulin	Hochwald and Wallenstein (1967)
Cat	20.9	-	I-125 Albumin	Weiss and Wertman (1978)
Dog	44.0	224	Inulin	Sahar et al. (1971)
Dog	53.0	-	^{14}C-Inulin	Oppelt et al. (1963)
Monkey	40.4	-	Blue Dextran	Martins et al. (1976)
Goat	164	143	Inulin	Heisey et al. (1962)
Calf	290	123	I-125 Albumin	Calhoun et al. (1967)
Man	350	13	I-125 Albumin	Cutler[a] et al. (1968)

Inulin (M.W. = 5200)

Blue Dextran (M.W. = 2 X 10^6)

Albumin (M.W. = 69,000)

reactions leading to the secretion of CSF by the choroid plexus. However, Macri *et al*. (1966) postulated that part of the effect of Diamox on CSF formation was mediated via the vascular system, since they observed choroidal arteriolar constriction with intravenous Diamox administration that was comparable to that produced by intravenous norepinephrine, both of which led to a reduction in CSF formation rate.

The effects of acidosis and alkalosis on CSF formation rates were studied by Oppelt *et al*. (1963) using a ventriculocisternal perfusion technique in adult dogs. They reported that acidosis induced by either 5-10% CO_2 inhalation, or by the intravenous administration of 0.1-0.3N HCl produced no significant effect on the CSF production rate. Metabolic alkalosis produced by intravenous infusion of 0.5N $NaHCO_3$ reduced CSF production 23% below control levels, whereas respiratory alkalosis (hyperventilation) resulted in a 46% reduction in CSF production rate. Ames *et al*. (1965) observed that inhalation of a 10% CO_2 gas caused marked dilation of the choroid plexus blood vessels and an increase in the rate of choroid plexus fluid formation which averaged 66% above control levels after 30 minutes and 40% after 1 hour of CO_2 exposure. They also observed that with hyperventilation there was a 68% drop in P_aCO_2 and constriction of the choroid plexus blood vessels which produced difficulty in obtaining fluid from the choroid plexus. They suggested that the effects of P_aCO_2 on CSF formation were secondary to its vascular effect and that the

rate-limiting factor in the formation of CSF is the blood supply to the choroid plexus. Pappenheimer also suggested that the rate of CSF formation may be limited by the blood supply to the choroid plexus (cited by Ames et al., 1963). Welch (1963) demonstrated that 25% of the plasma entering the rabbit's choroid plexus is converted into CSF.

There is further evidence that there is a relationship between cerebral blood flow and the formation rate of CSF in mammals. Snodgrass and Lorenzo (1972) found that CSF formation rates in cats were altered by 11% when rectal temperature increased or decreased by $1^{o}C$ within the range $31-41^{o}C$. They postulated that this effect was similar to that of temperature on cerebral blood flow. Rosomoff (1954) demonstrated that cerebral blood flow varies linearly with body temperature between the range $30-45^{o}C$, and that a $1^{o}C$ change produced a 6.7% change in cerebral blood flow. A more direct relationship was found by Bering (1959) in which he observed that changes in CSF formation rate correlated with both cerebral blood flow and cerebral oxygen consumption. Carey and Vela (1974) found that the reduction of systemic blood pressure which was sufficient to reduce cerebral blood flow also reduced CSF formation rates in dogs. These workers demonstrated that when systemic arterial blood pressure was reduced to 62 $\pm$ 1 mm Hg from control levels (119 $\pm$ 9 mm Hg) by hemorrhage, there was a significant reduction (40%) in CSF formation rate as measured using the inulin dilution technique. With the restoration of mean arterial

blood pressure by total replacement of blood volume, CSF production rate rose to approximately pre-hemorrhagic control levels. Weiss and Wertman (1978) reported that when systemic blood pressure was lowered to an extent at which cerebral perfusion pressure (CPP; mean arterial blood pressure minus intracranial pressure) fell below 55 mm Hg, CSF formation rate decreased. They found there was no difference in the CSF production rate due to variations in intracranial pressure or to systemic blood pressure for those animals in which CPP was maintained at levels greater than or equal to 70 mm Hg. They suggested that cerebral autoregulatory mechanisms could not maintain adequate choroidal blood perfusion when cerebral perfusion pressure was below 55 mm Hg.

2.2. Cerebrospinal fluid absorption

Early studies indicated that CSF moving from the cerebral ventricles to the subarachnoid spaces was being drained into the blood vascular system. Dandy and Blackfan (1914) and Frazier and Peet (1914) showed that when the aqueduct of Sylvius was blocked, internal hydrocephalus developed and there was an increase in intraventricular pressure. This suggested that the main CSF drainage route is distal to the aqueduct. Weed (1914) showed that fluid in the subarachnoid space was drained into the large endocranial venous sinuses via the arachnoid villi. He injected dyes into the subarachnoid space of dogs and found them in the

arachnoid villi and sagittal venous sinuses. Welch and Friedman (1960) showed histologically that the arachnoid villus in monkeys is a labyrinth of small interconnecting tubules which project into the lumen of the sinus. These investigators also excised pieces of dural membrane containing arachnoid villi and mounted the membrane so that it separated two fluid filled chambers. A pressure of 10 mm H_2O was observed to be the critical opening pressure which allowed fluid flow from the CSF side of the membrane to its perfused side. When sagittal pressure exceeded CSF pressure, fluid flow stopped. These authors concluded that the arachnoid villi act as unidirectional valves which permit the flow of CSF into the venous system while preventing the flow of blood in the opposite direction.

2.2.1. Quantitative measurement of cerebrospinal fluid absorption

Two in vivo techniques have been used to measure the rate at which molecules are removed from CSF: 1) intracisternal injection of test substances, and 2) perfusion of the ventriculocisternal system with an artificial CSF containing test molecules.

Davson et al. (1962) injected a measured volume of fluid (0.1 ml) which contained known concentrations of ^{24}Na, inulin and sucrose into the cisterna magna of anesthetized rabbits to determine the relative rates at which substances were removed from the subarachnoid space. One hour after injection, the total cranial volume of CSF (1.0-2.0 ml) was

withdrawn from the cisterna magna and analyzed for [24]Na, inulin and sucrose. The removal rate for different substances from the CSF system was determined by the difference in the amount of test substance injected into the CSF and the amount remaining in the withdrawn fluid at the end of 1 hour, expressed as a ratio of the amount injected. [23]Na was used as the reference substance and the removal of injected molecules from CSF were expressed as a percentage of [24]Na loss in which the relative rates of loss for [24]Na, sucrose and inulin were: 100%, 64% and 43%, respectively. Davson concluded that the slow loss of inulin from the CSF was due to its being removed only by bulk absorption from the subarachnoid space. The larger rate of loss of sucrose was due to its diffusion in the extracellular spaces of the brain in addition to its bulk absorption.

Pappenheimer _et al_. (1962) perfused the ventriculocisternal system of unanesthetized goats and estimated quantitatively a value for CSF absorption by calculating an inulin clearance from the CSF system. Inulin was assumed to be removed mainly by bulk absorption, since at a cerebroventricular pressure of -15 cm H_2O all inulin entering the lateral ventricles was recovered in the cisternal effluent. This indicates that inulin does not diffuse across the ventricular ependyma. They also observed that when intraventricular pressure was changed, inulin clearance varied linearly with pressure. This suggested that there was a direct relationship between the rate of bulk

fluid absorption and CSF hydrostatic pressure. Bulk
absorption of CSF varied from zero at an intraventricular
pressure of -15 cm H_2O to approximately 0.4 ml/min at an
intraventricular pressure of +30 cm H_2O. The technique of
ventriculocisternal perfusion has been employed in the
determination of CSF absorption in a variety of species and
with other high, molecular weight molecules. Anderson and
Heisey (1972) use the clearance of radio-iodinated human
serum albumin (RIHSA; M.W. = 65,000) as a measure of bulk
absorption rate in chickens, and showed that it was removed
from CSF by a pressure-dependent process which was comparable
to results found in monkeys, using blue dextran (M.W. = 2 X
10^6) as the non-diffusible indicator (Martins et al., 1976).

2.3. The quantitative measurement of molecular movement from
the CSF

Material is removed from CSF by several mechanisms:
bulk flow of fluid via the arachnoid villi into the blood,
diffusion of substances into nervous tissue or blood, and
active transport of substances into nervous tissue or blood.
Bulk absorption refers to the pressure-dependent removal of
CSF and its contents through the arachnoid villi. For
example, large molecules such as inulin (M.W. = 5200) and
dextran (M.W. = 70,000) leave the CSF system by a process
comparable to glomerular filtration in the kidneys (Heisey et
al., 1962). Since there is no filtration across the
arachnoid villi (Welch and Pollay, 1961; Davson, 1967),
clearance by bulk absorption is one mechanism for a substance

to leave the CSF system.

The passive or active (non-bulk) movement of substances into the blood can also account for the loss of some materials from the CSF system. Heisey et al. (1962) measured molecular movement of tritiated water (TOH), urea, creatinine and fructose from the CSF system using the ventriculocisternal perfusion technique. They perfused various test substances into the brain's ventricular system in goats and calculated the rate of molecular loss from the cerebral ventricles as a function of the difference between the total clearance of test substance and the amount lost through bulk absorption. They found that diffusional loss of test molecules from CSF was inversely related to the size of the molecule, in which TOH was greater than urea, creatinine and fructose, in terms of decreasing permeability. The transependymal efflux rates for these test substances were independent of CSF intraventricular pressure over the range -10 to +30 cm H_2O.

2.3.1. Molecular exchange between CSF, brain and blood during hypercapnia

Early studies using intravenously injected vital dyes demonstrated that although many body tissues stain, the brain is relatively free of staining, which provided the concept of blood-brain and blood-CSF barriers.

Breathing CO_2 (hypercapnia) appears to increase the permeability of the blood-CSF and blood-brain barriers to a variety of substances. Clemedson et al. (1958) found that

inhalation of 7-30% CO_2 caused staining of the brain parenchyma by intravascularly injected trypan blue, an acidic dye which does not normally penetrate the central nervous system (CNS). They further observed that hypercapnia in rabbits and guinea pigs produced more staining of the brain parenchyma than it did in cats. A longer exposure to CO_2 was necessary to produce trypan blue staining in the CNS in all animals using 7-10% CO_2 concentrations than when 11-30% CO_2 concentrations were used. These investigators demonstrated that there was no dye penetration if trypan blue was administered after the period of 7-30% CO_2 inhalation. This indicated that the abnormal permeability of the blood-brain barrier was rapidly reversible. Cutler and Barlow (1966) studied the uptake of labelled 125-I albumin in male guinea pigs breathing 10% or 25% CO_2 for periods of time varying from 5 minutes to 8 hours. They suggested that albumin entry into the brain was related both to the length of CO_2 exposure and to the elevation of $P_a CO_2$. They observed no labelled albumin in the brain parenchyma during metabolic acidosis produced by intravenous infusion of 0.1N HCL. Lending et al. (1961) found that inhalation of 7% CO_2 increased the rate of entry of intravenously injected 131-I albumin twenty times over its normocapnic levels into the cisterna magna fluid of puppies while only a four-fold increase was observed in the adult dogs over its normocapnic level. They attributed the differences in results between puppies and adult dogs to be due to the arterial pH and CO_2 contents produced in puppies

but which were not produced in the adult dogs.   Hochwald et al. (1973) reported that during steady-state perfusion of the ventriculocisternal system, 10% CO_2 inhalation in anesthetized cats caused more than an 11-fold increase in the amount of intravenously injected 125-I albumin into the brain ventricles.   With the removal of 10% CO_2 as the breathing gas mixture, the amount of 125-I albumin in the CSF came back approximately to normocapnic steady-state levels, indicating that the effect of hypercapnia on the blood-CSF barrier was reversible .

These permeability changes of the blood-brain and blood-CSF barriers observed during hypercapnia were observed to be related to the magnitude of elevated P_aCO_2 (Clemedson et al., 1958; Lending et al., 1961) but not following reduction of blood pH by acid infusion (Cutler and Barlow, 1966).   Elevation of blood PCO_2 causes vasodilation of the cerebral vasculature and an increase in cerebral blood flow (Wolff and Lennox, 1930; Kety and Schmidt, 1948; Reivich, 1964).   Cerebral blood flow has been shown to increase linearly with P_aCO_2 over the range 15 to 76 mm Hg (Smith et al., 1971; Grubb et al., 1974), but is not correlated with blood pH (Reivich, 1964).   Changes in cerebral vasculature hemodynamics during hypercapnia may be factors leading to the increased entry rate of substances into the brain and CSF since the effects of vascular permeability of the CNS were observed to be readily reversible when CO_2 inhalation was discontinued as the breathing gas mixture (Goldberg et al.,

1963; Hochwald et al., 1973).

2.4. Cerebrospinal fluid volume

Pappenheimer et al. (1962) introduced a method for estimating the volume of CSF during perfusion of the CSF system of goats with an artificial solution containing test molecules. They integrated the transient rise in molecular concentration as a function of time. Their method of estimating the distribution volume of a test molecule accounts for the total amount of material added to the system by perfusion inflow and subtracts from the amount recovered from perfusion effluent and the amount lost by clearance from the ventricles. It is assumed that the calculated steady state clearance rate occurred throughout the period of rising effluent concentration preceeding the steady state concentration. These investigators perfused the lateral ventricles to the frontal subarachnoid space and calculated the distribution volumes of inulin (22.7 ml), creatinine (26.0 ml), and Diodrast-I^{131} (25.3 ml) to be approximately equal to the total volume of fluid that can be drained from the goat's cranium. They also estimated the distribution volumes of these test substances in the perfused ventriculocisternal system. They found them to be slightly less than half of the total CSF volume; inulin (11 ml), creatinine (8.5 ml), and Diodrast-I^{131} (8.5 ml).

Other investigators have reported distribution volumes using Pappenheimer's method in other species and with

other test substances. Bering and Sato (1963) found for the anesthetized dog, that the distribution volume in the ventriculocisternal system was 3.0 ml for inulin and 5.2 ml for RISA (131-I serum albumin). They attributed the distribution volume to include the lateral, third, and the fourth ventricles, the subarachnoid space of the posterior fossa, and the cisterna magna. The combined volumes of the two lateral ventricles and the third ventricle calculated from ventriculo-aqueductal perfusions were 1.6 ml for inulin and 2.2 ml for RISA. Cutler[b] et al. (1968) perfused the ventriculocisternal system of kittens and adult cats with 125-I albumin. They recovered less than 2% of the total 125-I albumin from the brain, and suggested that the distribution volume of 125-I albumin represents the perfused compartment volume. They used a negative outflow pressure so that bulk fluid absorption was zero. They found distribution volumes of 0.84 ml and 0.75 ml in the kitten and adult cats, respectively. Sahar et al. (1970) measured the distribution volume of 131-I cat serum albumin in normal and kaolin-induced hydrocephalic cats and found correspondence between the calculated distribution volumes and the direct volume measurements of silicone rubber casts of the perfused space. These investigators found that the volume of the silicone cast made during ventriculocisternal perfusion at zero cm H_2O intraventricular pressure was 0.74 ml, a cast volume which included not only cerebral ventricles but some portion of the cranial subarachnoid space in which residual

casting material was found. They suggested that during ventriculocisternal perfusion in normal cats, the distribution volume (0.50 ml) measured at -8 cm H_2O represented only the cerebral ventricular volume and not that of the subarachnoid spaces. At higher perfusion pressure, they found an increase in measured volume which they attributed to perfusion fluid entering the subarachnoid spaces. This conclusion was supported by perfusions with silicone casting material, which also entered the subarachnoid space when perfusion pressure was high.

III. STATEMENT OF THE PROBLEM

The purpose of this study was to determine in anesthetized cats the effect of hypercapnia on cerebrospinal fluid (CSF) dynamics. The ventriculocisternal perfusion technique was used to establish steady-state concentrations of inulin and sucrose in the cerebral CSF compartments. Analysis of steady-state conditions, during both normocapnia and hypercapnia allowed deductions about the effect of hypercapnia on CSF absorption and formation rates as well as the molecular exchange between CSF and blood, and CSF and brain. Mathematical analysis of the transient approach to steady-state concentration of test molecules and the transient decrease in concentrations using a perfusion inflow free of test molecules provided information concerning the effects of hypercapnia on the volume of the cranial CSF compartment.

IV. MATERIALS AND METHODS

4.1. General operative procedures

Mongrel, male or female cats, Felis domesticus, weighing 3.0-4.5 kg were anesthetized with an intraperitoneal injection of Dial-urethane (0.6 ml per kg; Appendix E). A catheter (PE-60 tubing) was placed in the femoral artery for monitoring arterial blood pressure and for obtaining arterial blood samples for pH and PCO_2 measurements (Appendix A). A femoral venous catheter (PE-60 tubing) allowed for administration of anesthesia supplements and of a 0.9% sodium chloride drip to maintain hydration of the animal. The trachea was cannulated with a 1 cm diameter vinyl tube which was attached to a respiratory valve assembly for administering gas mixtures and connected to a pneumotachograph (Model 7324 Dynasciences, Bluebell, PA) for monitoring respiration. A heating pad was used to keep body temperature at $38^{\circ} \pm 0.5^{\circ}C$ which was continuously monitored using a rectal thermistor probe (Model 400 Tele-Thermometer, Yellow Springs Instrument Co., Yellow Springs, Ohio) placed 10 cm beyond the anal sphincter.

4.2. Brain ventricular and cisternal puncture

The animal's head was secured in a stereotaxic frame (Model 1430, David Kopf Instruments, Tujunga, CA), by infra-orbital and serrated palate clamps and ear bars inserted into the external auditory meatus. A 4 cm long incision was made through the skin of the head from a point 4 cm from the supraorbital ridge to extend posteriorly to a point 1 cm behind a line posterior to the near dege of the ear margin. Skin, subcutaneous fascia, and muscle were retracted to expose a 3 cm^2 area of skull surface. Using a 2 mm diameter dental burr, two 4x4 mm holes were drilled through the skull 13.5 mm anterior to the ear bars and 2.5 mm lateral from the animal's cerebral midline. Two ventricular cannulae (Figure 1) which were connected to a motor driven syringe pump (Model 940, Harvard Apparatus Co., Dover, MA) and to a pressure transducer (Model P23C. Grass Instrument Co., Quincy, MA) for recording CSF pressure were lowered separately through the holes drilled in the skull and through brain matter until the probe tips penetrated the lateral cerebral ventricle. Communication with the cerebral ventricles was indicated by a drop in the CSF pressure as the probes penetrated the walls of the lateral ventricles. Figure 2 shows the arrangement of the apparatus used for the ventriculocisternal perfusion experiments.

A single cisternal needle (21 ga.; metal hubless needle) held in a micromanipulator (Model MM-3; Eric Sobotka Co., Inc., Farmingdale, NY) was positioned with its point on the atlanto-occipital membrane at the midline, midway between

Figure 1.   The drawing is a cross-sectional view of the
lateral ventricular cannula assembly which is
attached to a stereotaxic electrode carrier
(Model 1460, David Kopf Instrument, Tujunga, CA)
by the carrier bar (A). A brass block (E) is
drilled to accept two pieces of 23 ga. needle
tubing (B+C) and 21 ga. needle tubing (D) which
are press fitted and soldered to the block.
Polyethylene tubing (PE-50) from a syringe-drive
pump is attached at (B) and to a pressure
transducer for measurement of intraventricular
pressure (C). A 1 mm diameter glass capillary
used to make the probe (F) is sharpened and heat
sealed using a vertical micropipette puller
(Model 700B, David Kopf Instrument). Holes in
the side of the glass probes are made under
magnification by grinding with a fine grit
rotary wheel. The glass cannula is cemented
(Devcon, 5-min epoxy) onto the 21 ga. needle
tubing (D).

FROM PUMP →

TO PRESSURE TRANSDUCER →

STEEL

BRASS

EPOXY

GLASS

A

B

C

D

E

F
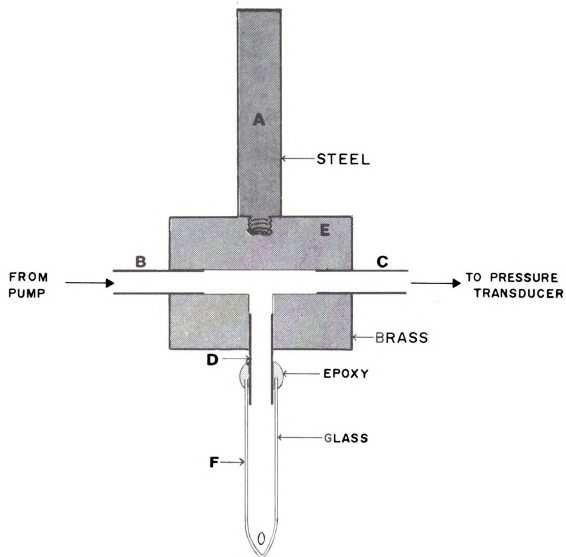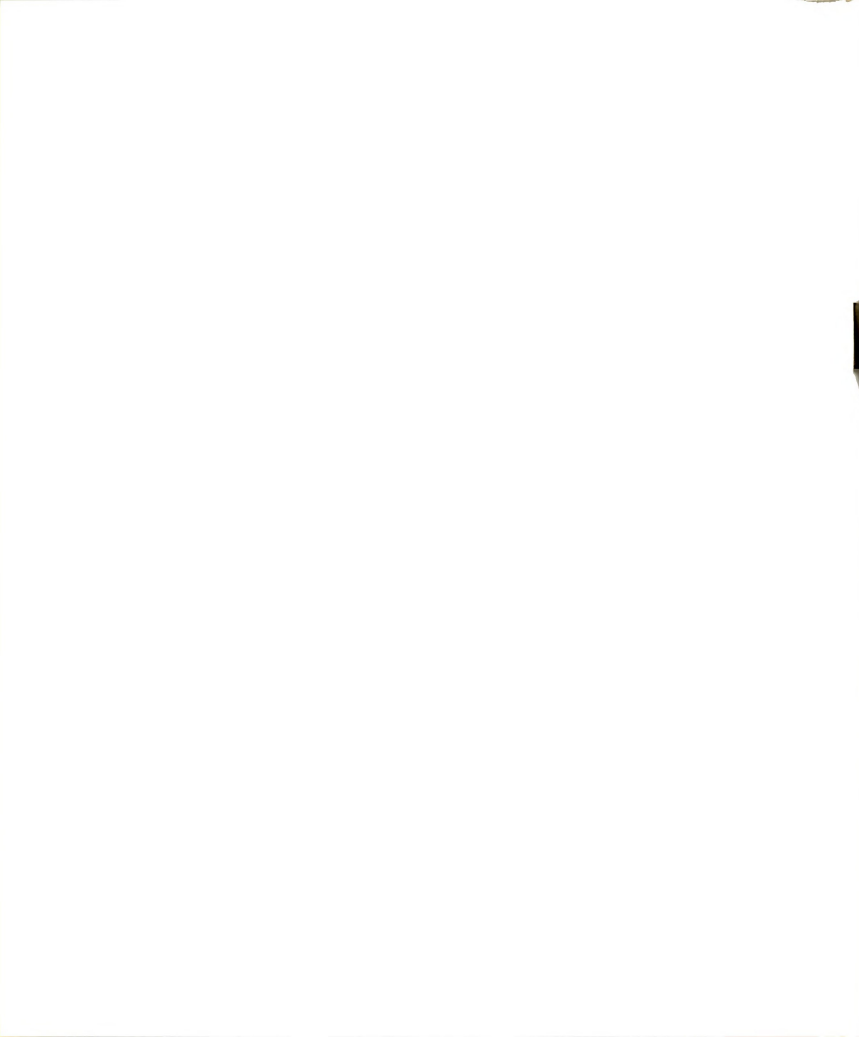
FIGURE 1

Figure 2. Schematic of the experimental preparation for cerebral ventricular perfusions. The head of an anesthetized cat is secured in a stereotaxic frame while an artificial cerebrospinal fluid (CSF) is perfused through the lateral cerebral ventricle. CSF inflow rate ($\dot{V}_i$) is controlled by a syringe-drive pump (Model 940, Harvard Instrument Co., Dover, MA). CSF ventricular pressure is continuously monitored through a pressure transducer (Model P23C, Grass Instrument Co., Quincy, MA). With a cannula inserted into the cisterna magna, outflow rate ($\dot{V}_o$) is measured using a drop counter (Model PTT1, Grass Instrument Co.) and samples of CSF are collected for weighing and for analysis of tracer molecules. The animal inspired either room air or an 8-10% CO_2 in room air mixture through a valve assembly attached to its tracheal cannula, from which respiratory activity was monitored using a pressure transducer. Arterial blood pressure was monitored by means of a femoral arterial cannula connected to a pressure transducer (not shown).
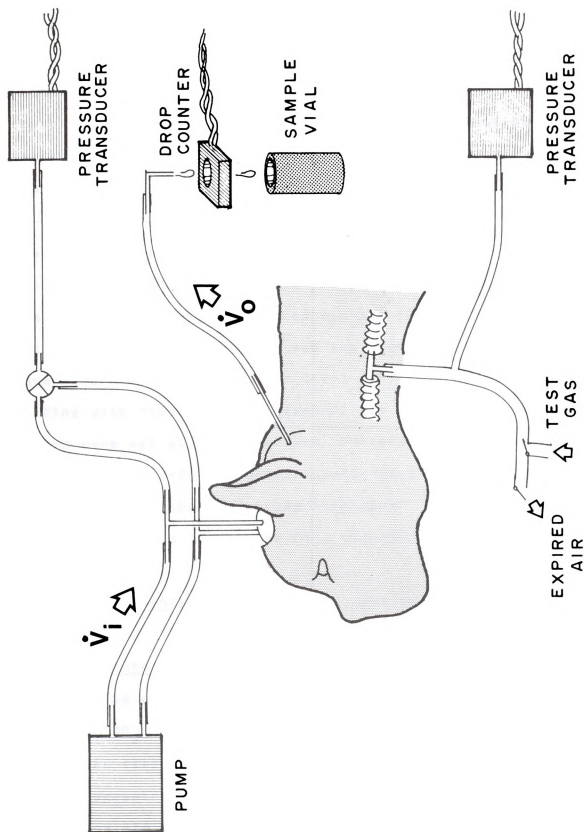
FIGURE 2

the atlas and the base of the skull and in a plane parallel to the stereotaxic frame. A 50 cm length of polyethylene tubing (PE-90) was attached to the needle as the outflow cannula. The needle was advanced approximately 8 mm to puncture the atlanto-occipital and dural membranes and then withdrawn slowly until CSF could be withdrawn freely through the outflow cannula

Ventricular perfusion was begun using an artificial cat cerebrospinal fluid (CSF), the electrolyte composition of which is reported in Appendix D. The outflow cannula was positioned in a photocell drop counter (Model PTT1, Grass Instrument Co., Quincy, MA) and the ventricular hydrostatic pressure was adjusted by the level of the cisternal outflow tubing with repect to the level of the stereotaxic ear bars which were set at zero pressure. Arterial blood pressure, respiration, perfusion outflow rate and ventricular pressure were monitored throughout the experiment using a polygraph (Model 5P, Grass Instrument Co., Quincy, MA).

4.3. Experimental perfusion with test molecules

4.3.1. Protocol A.

The animal inspired either room air (normocapnia) or an 8-10% CO_2 in air gas mixture (hypercapnia) while the CSF perfusion fluid was substituted with another, containing known concentrations of inulin and tritiated sucrose. After approximately 30 minutes of perfusion during either

normocapnia or hypercapnia, a steady-state concentration of
test molecules in the cisternal effluent was reached. At 60
minutes, the inspired gas was changed to either room air or
8-10% CO_2; opposite of the mixture used initially. Perfusion
of the ventricular system continued for an additional 30
minutes at which time the CSF perfusion fluid was changed to
one containing inulin and ^{14}C labelled sucrose, and perfused
for an additional 60 minutes. Data from a representative
experiment are shown in Figure 4 (Section 5; Results).

4.3.2. Protocol B.

Perfusion experiments were similar to those described
in Protocol A, time prior to 60 minutes, using inulin,
radiolabelled sucrose and dextran (New England Nuclear,
Boston, MA) as test molecules. After steady state
concentrations of test molecules in the cisternal effluent
were achieved the inflow perfusion fluid was changed to one
containing no test molecules and perfusion continued for an
additional 60 minutes under the same breathing condition
(normocapnia or hypercapnia). In some animals, the entire
experiment was repeated but under the alternate respiratory
condition (room air or 8-10% CO_2). These experiments lasted
approximately 120 minutes for each respiratory condition or a
total time of 240 minutes if both breathing conditions were
achieved in the same animal. Representative data from one
such experiment in which the animal breathed room air only is
shown in Figure 5 (Section 5; Results).

4.4. Experimental criteria

Following every ventriculocisternal perfusion experiment, a methylene blue solution was perfused for ten minutes through the ventricular needles to confirm cannula placements. The animal was killed with an intravenous injection of sodium pentobarbital, the skull was removed, and the ventricles were examined for methylene blue stain. The appearance of methylene blue staining on the cortex would suggest perfusion had occurred other than in the ventriculocisternal spaces. This precluded using data from that experiment. When an excessive amount of blood was found in the cisternal effluent samples during the perfusion experiment, data from that experiment were not used.

Steady state measured and calculated data were selected from perfusion experiments on the basis of two experimental criteria: 1) the fluid mass balance equation ($\dot{V}_i + \dot{V}_f = \dot{V}_o + \dot{V}_a$) was satisfied and 2) variances of test molecule concentrations in the perfusion effluent were less than or equal to 0.0010. Data which did not meet these two criteria were not used in this study.

4.5. Measurement of perfusion inflow and outflow rates and concentrations

The inflow and outflow rates of ventriculocisternal perfusion were determined gravimetrically for each experiment by collecting CSF effluent over timed periods in tared vials. The inflow concentraion of test molecules was determined by

analysis of an aliquot from the inflow syringe and outflow
concentrations were determined similarly from measured drops
of the cisternal effluent. Concentrations of radio-labelled
sucrose and dextran were analyzed using a liquid
scintillation counter (Model 3150P, Beckman Instruments,
Fullerton, CA), (Appendix B). Inulin concentrations were
determined colorimetrically by the resorcinol method without
alkali treatment (Appendix C).

4.6. Mathematical analysis and calculations

Principles and equations used in the calculation of
bulk absorption rate, CSF formation rate, and the
transependymal efflux rate have been previously described
(Pappenheimer et al., 1961; Heisey et al., 1962) and are
presented below.

4.6.1. Definition of symbols:

$\dot{V}$ = volume flow rate (μl/min)

i,o = subscripts denote inflow and outflow volumes or
concentrations

f,a = subscripts refer to bulk formation and
absorption of CSF, respectively.

c = concentration (quantity/μl)

$\bar{c}_v$ = exponential mean concentration in the
ventricular system.

= $c_i - c_o / \ln(c_i/c_o)$ (quantity/μl)

when c_i = 0, the function above is undefined

and $\bar{c}_v$ was calculated as: $c_o + 0.37(c_i-c_o)$ as described by Pappenheimer et al. (1961).

$\dot{n}_x$ = steady-state transport of any substance, x, from or into the CSF perfusion system = $\dot{V}_i c_i - \dot{V}_o c_o$ (quantity/min).

F_x = clearance of x = $\dot{n}_x/c$. c may be chosen as $\bar{c}_v$ or c_o depending upon whether one evaluates clearance from the ventricular system or from fluid reabsorbed distal to the fourth ventricle (μ l/min).

K = efflux coefficient of any substance, x, from the perfusion system by means other than bulk absorption (μl/min)

4.6.2. Rate of bulk absorption, $\dot{V}_a$

Heisey et al. (1962) determined that the ependymal linings of the ventricular system are virtually impermeable to inulin. The inulin lost from the CSF system can be accounted for by bulk fluid absorption distal to the fourth ventricle since the rate of inulin lost varies linearly with the hydrostatic pressure in the CSF system (Heisey et al., 1962).

$$\dot{V}_a = (\dot{V}_i c_i - \dot{V}_o c_o)/c_o = \text{clearance of inulin, } F_{in} \qquad (1)$$

where c's are inulin concentrations.

4.6.3. Rate of cerebrospinal fluid formation, $\dot{V}_f$

The diffusion of inulin from the ventricular system into brain tissue is negligible (Heisey et al., 1962; Rall et al., 1962), therefore any dilution of inulin during passage through the ventricles results from newly-formed inulin-free fluid by the animal.

$$\dot{V}_f = \dot{V}_i (c_i - c_o)/c_o \qquad (2)$$

where c's are inulin concentrations

4.6.4. Efflux coefficient, K (non-bulk clearance)

The total clearance of molecules from the CSF system which are smaller than inulin or dextran and are not present in significant concentrations in blood has two components: (1) the clearance due to diffusion and/or active transport, and (2) clearance due to bulk absorption. The clearance of the small molecule by bulk absorption is given by:

$$F_B = F_{in} \left[\frac{c_o}{\bar{c}} \right]_x \qquad (3)$$

where:

$\left[\dfrac{c_o}{\bar{c}} \right]_x$ = ratio of the cisternal outflow and exponential mean ventricular of the small molecule, x.

F_{in} = inulin clearance

F_B = clearance of x by bulk absorption

Subtracting the bulk absorption clearance of x from its total clearance yields clearance due to diffusion or active transport.

$$K = F_x - F_B \tag{4}$$

where:

K = efflux coefficient of x ($\mu l/min$)

4.6.5. Volume of distribution, V_D

The distribution volume is determined by numerically integrating the transient rise of molecular outflow concentration to the steady-state with respect to time.

$$V_{D_x} = \frac{\sum_{j=1}^{n} \left[\dot{V}_i c_i - \dot{V}_{oj} c_{oj} - F_x \bar{c}_j \right] \Delta t_j}{c} - V_{ds} \tag{5}$$

where:

V_{Dx} = distribution volume of x (μl)

$\dot{V}_i$ = perfusion inflow rate

c_i = perfusion inflow concentration

$\dot{V}_{oj}$ = perfusion outflow rate associated with the jth

sample.

c_{oj} = perfusion outflow concentration of the jth

sample.

F_x = steady state clearance of the test molecule

Δt_j = outflow collection time between the j-1st and

jth sample in minutes

$\bar{c}_j$ = mean concentration of x in the CSF during the

jth sample.

$c = \bar{c}$, steady-state mean ventricular concentration

for molecules smaller than inulin.

$= c_o$, steady state outflow concentration for

inulin.

n = total number of samples

V_{ds} = volume of the perfusion needles and tubing

(dead space volume).

j = first outflow sample beginning at time zero

= or first outflow sample after time zero was

adjusted (Appendix F) in which dead space

volume was omitted.

4.7. Statistical analysis

All data were analyzed statistically with a 0.05
probability criteria, using the Student's "t" (paired and
group comparisons) or the analysis of variance tests on group
comparisons (Sokal and Rohlf, 1969). Statistical comparisons
were made using a programmable calculator (Model 67,
Hewlett-Packard, Corvallis, Oregon) and a mini-computer

(PDP-11, Digital Equipment Corp., Maynard, MA).

4.7.1. Optimization routine

The mean steady-state concentration for each test molecule was determined statistically by a direct search method called the Pattern Search routine (Gottfried and Weisman, 1973). This method evaluates the linear path of steady-state concentrations by calculating a summated variance and mean for every molecular concentration in that path, starting with the concentration at the longest perfusion time and sequentially working backward in time. The criterion for determining an optimum mean steady-state concentration for any molecule is to find the series of concentrations with the smallest calculated variance until the largest constant step increase in variance is encountered.

4.7.2. Non-linear curve analysis

Transient data obtained during the "washout" phase of the perfusion experiments (Protocol B) were fitted by a multiple exponential equation by the method of non-linear least squares (Appendix F). The criterion for a "good fit" of experimentally observed points to exponential equations, was evaluated by a chi-square test (Equation F-2; Appendix F).

V. RESULTS

5.1. Effects of hypercapnia on arterial pH and PCO_2

These experiments were designed to study the effects of increased brain blood flow on cerebrospinal fluid formation ($\dot{V}_f$), absorption ($\dot{V}_a$) and on brain ventricular permeability (K). Carbon dioxide inhalation was used to increase P_aCO_2 because it is known to cause cerebral vasodilation and an increase in brain blood flow. Data reported in Table 2 show that in 18 animals spontaneously breathing room air, P_aCO_2 was 28 mm Hg but it increased to 54 mm Hg when the inspired gas was an 8-10% CO_2-in-air mixture. In addition, arterial pH decreased significantly ($P < 0.05$) from 7.33 during room air breathing to 7.11 when the animal breathed the CO_2 mixture, indicating a significant respiratory acidosis.

5.2. Effects of hypercapnia on steady state CSF dynamics

Successful ventriculocisternal perfusions as judged by the criteria outlined in Section 4.4 were obtained in 18 cats breathing room air and 11 cats breathing 8-10% CO_2. Measured steady state data are reported in Table G-1 (Appendix G) for animals used in Protocol A and Protocol B

experiments (Methods; Sections 4.3.1. and 4.3.2.). In 9 of the 11 cats where comparisons can be made between room air and CO_2 breathing, the most consistent finding was an increase V_o during the period of CO_2 breathing. This agrees with data reported in Figure 3. Hypercapnia caused a decrease in the steady state outflow concentration (C_o/C_i) of inulin in 4 animals and of sucrose in 6 animals. This is consistent with data for dextran and sucrose reported in Figure 5. There was no consistent pattern of change in the intraventricular pressure (CSFP) between air and CO_2 breathing and no change in this parameter is seen in the representative data reported in Figure 3. Arterial pH and PCO_2 values in these animals were similar to those reported in Table 2.

Calculated parameters derived from the measured quantities reported in Table G-1 are shown in Table G-2 (Appendix G). The mean values for $\dot{V}_f$, $\dot{V}_a$ and K_{suc} determined in animals breathing air were not significantly different (P>0.05) from those breathing 8-10% CO_2. In addition, the resistance to bulk absorption, calculated as the ratio of intraventricular pressure (CSFP) to the bulk absorption rate ($\dot{V}_a$), was not significantly different (P>0.05) under the two respiratory conditions. The increase in $\dot{V}_o$ (Table G-1; Figure 3) is not apparently caused by an increased resistance to bulk absorption. In some cases, the level of the outflow cannula (which determines cerebroventricular pressure in the perfused system) was such that bulk absorption was zero which

causes absorption resistance to be undefined.

The mean values for $\dot{V}_f$ and K_{suc} reported in Table G-2 (Appendix G) did not show significant differences between air breathing and CO_2 breathing animals whether analysis was for means for all animals or for those exposed to both respiratory conditions. However, some animals showed marked increases in $\dot{V}_f$ during hypercapnia compared to the air breathing period. Weiss and Wertman (1978) showed that rate of CSF formation was affected by cerebral perfusion pressure (CPP) which they defined as the difference between mean arterial blood pressure (MABP) and cerebroventricular pressure (CSFP). We found that in 5 of the animals reported in Table G-2 which were exposed to both air and CO_2 breathing, CPP was maintained throughout the experiment at 68 mm Hg or higher. Data from these animals are shown in Table 3. Rate of CSF formation ($\dot{V}_f$) increased significantly (P<0.05) from 17.9 μl/min during air breathing to 35.4 μl/min during CO_2 breathing. The K_{suc}, which is a measure of non-bulk clearance of sucrose from the cerebral ventricles, also increased signficantly from 7.7 μl/min to 23.4 μl/min in response to hypercapnia. In 3 of the animals (Cat# 8, 12 and 13) the air breathing period preceeded the CO_2 breathing period while in the others (Cat# 17 and 22) the hypercapnic period was first. This indicates that the changes in $\dot{V}_f$ and K_{suc} were independent of experimental time and not due to "preparation deterioration". In addition, hypercapnia produced a significant increase (P<0.05) in $\dot{V}_o$ in these 5

animals, but $\dot{V}_a$ and the absorption resistance were not changed (P>0.05) significantly.

5.3. Effects of hypercapnia on intracranial fluid volumes

Data reported in Figure 3 are representative of responses of $\dot{V}_o$ and CSFP to hypercapnic induction and withdrawal. Steady state CSF pressure was not different under the two breathing conditions, but $\dot{V}_o$ was elevated during CO_2 breathing when compared to that during air breathing (see also $\dot{V}_o$'s in Table G-1 and Table 3). Data in Figure 3 show, in addition, transient changes in $\dot{V}_o$ and CSFP to hypercapnia induction and withdrawal. Both $\dot{V}_o$ and CSFP rose transiently during hypercapnia induction (time=60 min), the rise in pressure lasting a shorter time (3 minutes) than the rise in $\dot{V}_o$, the latter returning to steady state levels in approximately 6-7 minutes. The change in response to CO_2 withdrawal (Figure 3; time=156 min) was a transient fall in CSFP accompanied by a very dramatic slowing in $\dot{V}_o$. These data are interpreted to indicate a shift in intracranial fluid volumes and/or a transient change in CSF secretion during hypercapnia induction and removal. In addition to causing an increased brain blood flow, hypercapnia may also increase brain blood volume. Since the skull is a rigid container the increase in brain blood volume causes a competitive displacement of CSF volume through the relatively low resistance cisternal needle.

Data reported in Figure 4 show the steady state and

transient changes in cisternal effluent concentration observed during air and CO_2 breathing. The steady state sucrose concentration in cisternal effluent (C_o/C_i) was 85% and 74% of perfusion inflow concentration during the air and CO_2 breathing periods, respectively. Similar changes in effluent sucrose concentration were observed in all animals reported in Table 3. Data reported in Figure 4 show that hypercapnia induction caused a transient fall in the cisternal effluent concentration of sucrose. A transient reduction in perfusion effluent concentration of the test molecules was observed in every animal in which perfusion of the ventriculocisternal system with CSF containing inulin and/or sucrose was continued during the period of hypercapnic induction. These data, as well as those reported in Figure 3, indicate that a transient increase in $\dot{V}_f$ occurred during hypercapnia induction which caused a dilution of the test molecules. An alternative explanation is that a CSF volume free of test molecules is mixed with the perfused CSF compartment as a result of the expansion of brain blood volume and consequent reduction of cranial CSF volume. This results in a dilution of perfusion effluent concentrations.

5.3.1. Effect of hypercapnia on intracranial CSF volume

The volume of the perfused ventriculocisternal system was calculated from the molecular distribution volumes of ^3H and ^{14}C-labelled sucrose in animals breathing both room air and 8-10% CO_2. Distribution volumes were calculated by

integrating cisternal effluent concentrations as a function

of time (Figure 4). Two different methods were used to

calculate distribution volume. In Protocol A (Methods) the

numerical integration was performed after which the volume of

the perfusion cannulae (dead space) was subtracted from the

calculated volume (Methods; Section 4.6.5.). In the other,

using Protocol B (Figure 5), a curve fitting routine

(Appendix F) was used to analyze the transient decrease of

molecular concentrations (time 63-120 min; Figure 5) to fit a

general washout equation. The intersection of the generated

washout curve with the steady state concentration resulted in

the determination of a time lag due to the dead space of the

perfusion cannulae (Figure F-2; Appendix F). This time was

subtracted from the initial perfusion time zero. From this,

a distribution volume was calculated from the transient

approach of effluent molecular concentations to its steady

state (time 3-15 min; Figure 5).

Data presented in Table 4 show the comparisons of

sucrose distribution volumes in animals breathing both air

and CO_2. Distribution volumes for cats DS4 and DS6 were

calculated using the "time lag" method (Appendix F) while the

other cats were calculated using Equation 5 (Methods; Section

4.6.5.). There was no apparent difference in volume,

determined by the two methods and there was no significant

difference ($P>0.05$) in sucrose distribution volume between

air and CO_2 breathing. The distribution volume for inulin

(not shown) showed no difference ($P>0.05$) between animals

breathing room air (593 ± 32 µl in 8 cats) to those breathing
8-10% CO_2 (726 ± 79 µl in 4 cats). These data indicate that
the distribution volume (approximately 600 µl), which
represents largely the volume of the cerebral ventricles, was
not changed significantly by CO_2 breathing. Also there was
no significant difference ($P>0.05$) between sucrose and inulin
distribution volumes indicating that the method for
estimating a perfused volume is independent of test
molecule's weight and size.

5.4. Effects of hypercapnia on molecular distribution volume using compartmental analysis

Data reported in Figure 5 show the steady state and
transient changes in sucrose and dextran concentrations in
cisternal effluent. The steady state concentrations in
cisternal effluent were 85% and 78% of perfusion inflow
concentration for dextran and sucrose, respectively. These
are similar to molecular concentrations observed for inulin
and sucrose reported in Table G-1 (Appendix G). After steady
state concentrations were attained in the cisternal effluent,
an artificial CSF free of the test molecules was infused into
the ventriculocisternal system (time=60 min). This resulted
in a subsequent washout of the test molecules from
CSF-containing spaces (time 60-120 min). The transient
washout data for sucrose and dextran were mathematically
analyzed using a curve fitting routine (Appendix F) and are
described by a double exponential equation (Equation F-3;
Appendix F) indicating that the CSF perfusion system is a two

compartment system. The evaluation of the best exponential fit between the predicted curve ($Y(t) = Ae^{-k_1 t} + Be^{-k_2 t}$) and the experimental data was by the chi-square minimization test (Equation F-2; Appendix F). For the exponential curve to be judged as a good fit to the experimental data points in the present study, the chi-square value must be less than or equal to 0.0005.

Data presented in Table 5 show the coefficients and rate constants of a double exponential washout equation obtained by non-linear curve stripping technique in animals breathing room air (Table 5A) and 8-10% CO_2 (Table 5B). These data which indicate the washout of test molecules from a two compartment system is presumed to be from the cerebral ventricles and the subarachnoid space (based on the positions of the perfusion cannulae). Analysis of the rate at which test molecules are being removed from each compartment can indicate the relative volume of each CSF compartments during air and CO_2 breathing. From this, it was found that there were no significant differences ($P > 0.05$) detected in mean values of coefficients and rate constants between animals breathing room air and those breathing CO_2. Also, there were no significant differences ($P > 0.05$) in washout rates between the two different size molecules indicating that the removal rates of sucrose and dextran from CSF-containing spaces were independent of molecular weight, size and breathing stimulus. These data suggest that the volumes of the two compartments are not altered significantly by hypercapnia. This does not

support the hypothesis of a reduced intracranial CSF volume induced by hypercapnia as suggested by data in Figure 3. However, the double exponential equations derived from the washout data may only be describing apparent volume changes and not functional, anatomical changes of the CSF compartments between air and CO_2 breathing, since our data do not show a well mixed perfused system as indicated by the transient decrease in outflow concentration in all test molecules when the animal initially breathed CO_2 (Figure 4). This may cause misinterpretation of the washout data in reference to volume changes of either the cerebral ventricles or the subarachnoid space under air and CO_2 breathing if an unmixed compartment exist.

Table 2. Effect of hypercapnia on arterial pH and PCO_2

No. cats	Inspired gas mixture	pH	P_aCO_2 (mm Hg)
18	room air	7.33 $\pm$.02	28.3 $\pm$1.6
17	8-10% CO_2	7.11* $\pm$.02	53.8* $\pm$1.9

Mean $\pm$ SEM

* (P<0.05) room air $\neq$ 8-10% CO_2

Table 3. CSF dynamics during room air and 8-10% CO_2 breathing in animals with cerebral perfusion pressure greater than or equal to 68 mm Hg.

Cat#	room air					8-10% CO_2				
	$\dot{V}_a$ (μl/min)	$\dot{V}_o$ (μl/min)	$\dot{V}_f$ (μl/min)	K_{suc} (μl/min)	R (cm/μl·min⁻¹)	$\dot{V}_a$ (μl/min)	$\dot{V}_o$ (μl/min)	$\dot{V}_f$ (μl/min)	K_{suc} (μl/min)	R (cm/μl·min⁻¹)
8	16.5	158	30.5	9.2	0.3	0	194	48.0	44.3	u
12	3.2	155	14.2	7.8	1.6	0	187	39.9	29.3	u
13	11.5	154	20.5	5.0	0.6	10.5	174	39.5	9.0	0.7
17	0	150	4.3	14.8	u	5.2	155	16.2	14.7	0.8
22	16.2	143	20.2	1.5	0.4	27.5	146	33.5	19.7	0.2
Mean	9.5	152	17.9	7.7	0.7	8.6	171*	35.4*	23.4*	0.5
+SEM	3.4	2.6	4.3	2.2	.3	5.1	9.2	5.3	6.2	.3

*(P<0.05) room air ≠ 8-10% CO_2

u = undefined

R = resistance to CSF absorption

Figure 3. Data from a representative ventriculocisternal perfusion experiment (Cat# 10) showing the transient effects of hypercapnia induction and removal on cisternal outflow rate and intraventricular pressure. Perfusion inflow rate ($\dot{V}_i$) was held constant (144 μl/min) by a syringe drive pump. Outflow rate ($\dot{V}_o$; μl/min; closed circles; left ordinate) and cerebral ventricular pressure (CSFP; mm H_2O; open circles; right ordinate) are plotted as a function of time (minutes; abscissa). From 0-60 minutes the animal breathed room air; from 60-165 minutes, 8% CO_2; from 165-240 minutes, room air. With induction of hypercapnia (time=60 min) there was a transient increase in CSFP from 3 to 6 cm H_2O and a return to the pre-hypercapnic level within 3 minutes. Accompanying this transient rise in CSFP, $\dot{V}_o$ increased from 152 to 234 μl/min and returned to a slightly elevated rate in 6-7 minutes. When the hypercapnic stimulus was removed (time 165) CSFP and $\dot{V}_o$ decreased transiently and returned to their normocapnic values. The steady state $\dot{V}_o$ during hypercapnia was greater (166 μl/min) than during the 2 periods of room air breathing. These data are interpreted to indicate a competitive displacement of CSF by an increase in cerebral vascular volume during hypercapnia induction and an expansion of CSF volume when the hypercapnic stimulus is removed.
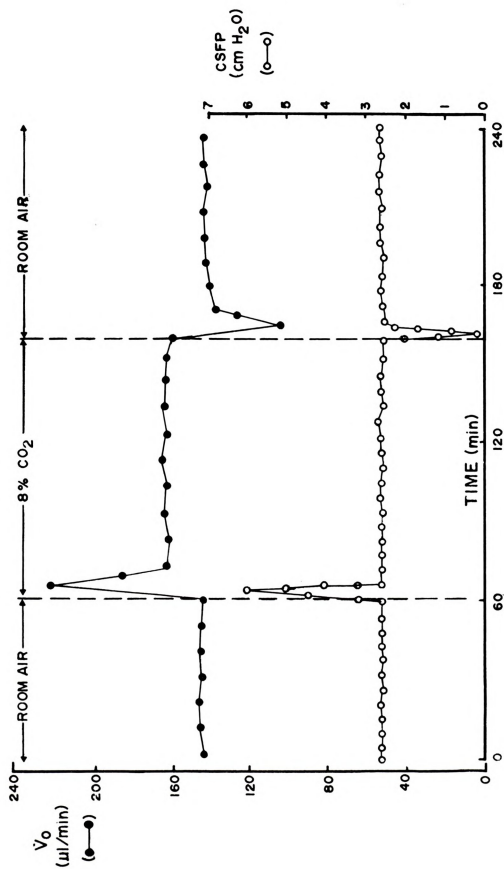
FIGURE 3

53

Figure 4. Results of a single ventriculocisternal perfusion experiment (Cat# 13) under both room air and CO_2 breathing conditions. The ordinate is the sucrose concentration in cisternal effluent expressed as a percentage of that in the perfusion inflow. The abscissa is time in minutes. At zero time, ^{3}H-labelled sucrose (closed circles) was added to the perfusion inflow. A transient rise to a steady state concentration was obtained in the cisternal outflow samples. At 60 minutes, the inspired gas was changed from room air to one of 8.1% CO_2 in air mixture resulting in a transient decrease in the cisternal effluent concentration of sucrose. At 80 minutes, the inflow perfusion fluid was changed to one containing ^{14}C-labelled sucrose (open circles) which resulted in a second transient rise of outflow concentration to a steady state and a fall in the outflow concentration of ^{3}H-labelled sucrose. The steady state concentrations of sucrose was higher under room air breathing conditions than when the animal breathed CO_2.
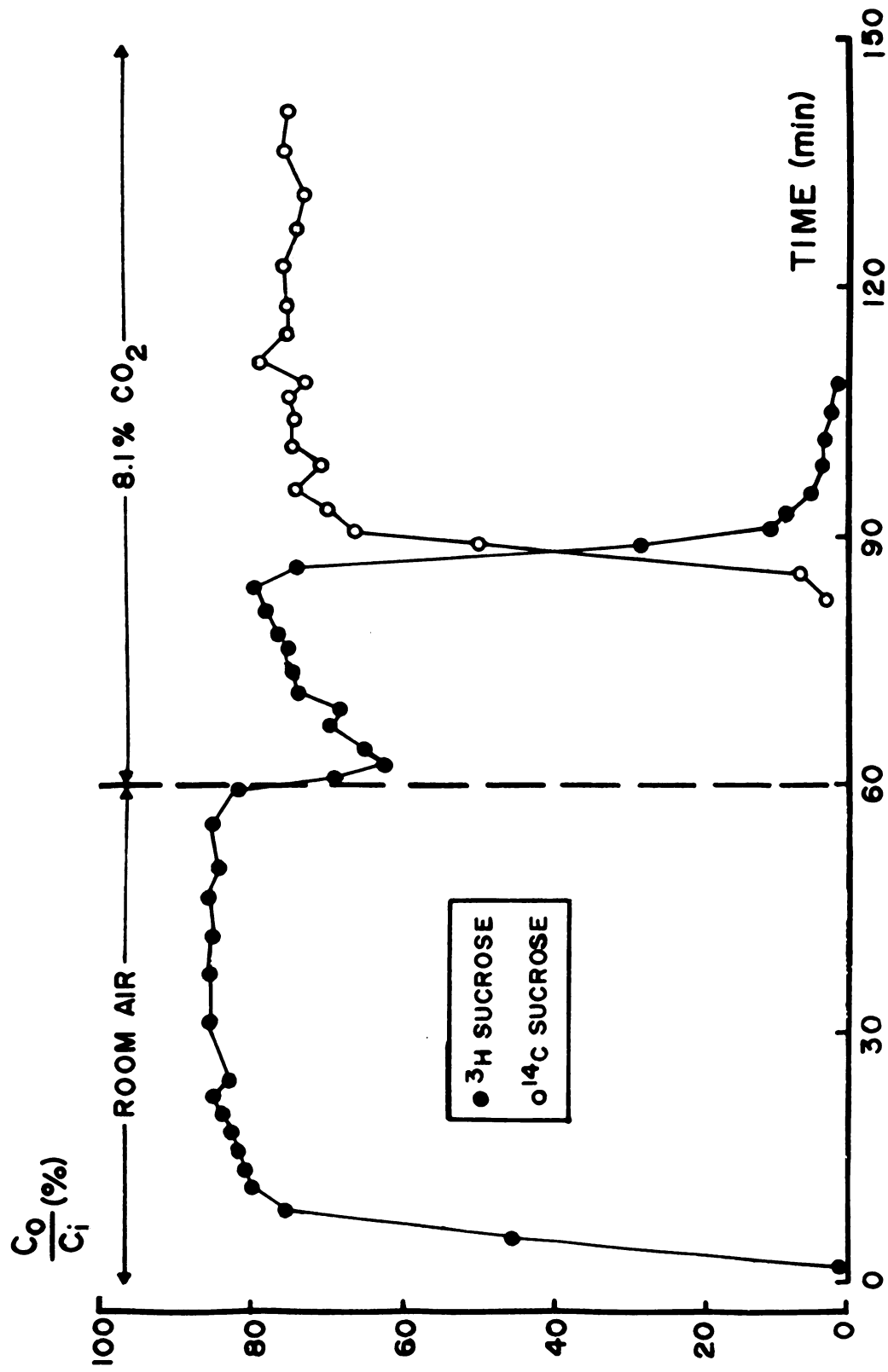
FIGURE 4

Table 4. ^3H and ^{14}C-labelled sucrose distribution volumes (V_D) of the
ventriculocisternal system during room air and 8-10% CO_2 breathing

	V_D (μl)	
Cat#	room air	8-10% CO_2
12	539	634
13	576	480
17	335	560
22	764	390
23	692	765
*DS 4	596	758
*DS 6	621	654
Mean	589	606
+SEM	51	53

* initial time lag was omitted by non-linear curve stripping technique
  (Appendix F)

Figure 5. Diagram showing representative data from a single ventriculocisternal perfusion experiment (Protocol B; Cat# 26). The ordinate shows the outflow concentration expressed as a percentage of the perfusion inflow concentration for the test molecules, ^{14}C-dextran (closed circles) and ^{3}H-sucrose (open circles). The abscissa is time in minutes. At zero time, an artificial cerebrospinal fluid which contained dextran and sucrose was perfused through the ventricular needles. There was no detectable concentration of the test molecules in the cisternal effluent at this time because of their initial and transient distribution within the ventricular and cannulae spaces. As the perfusion proceeded, the concentration of test molecules in the cisternal samples increased, eventually reaching a steady state concentration. At 60 minutes, the inflow perfusion fluid was changed to one containing no test molecules which resulted in a transient washout of the CSF-containing spaces.
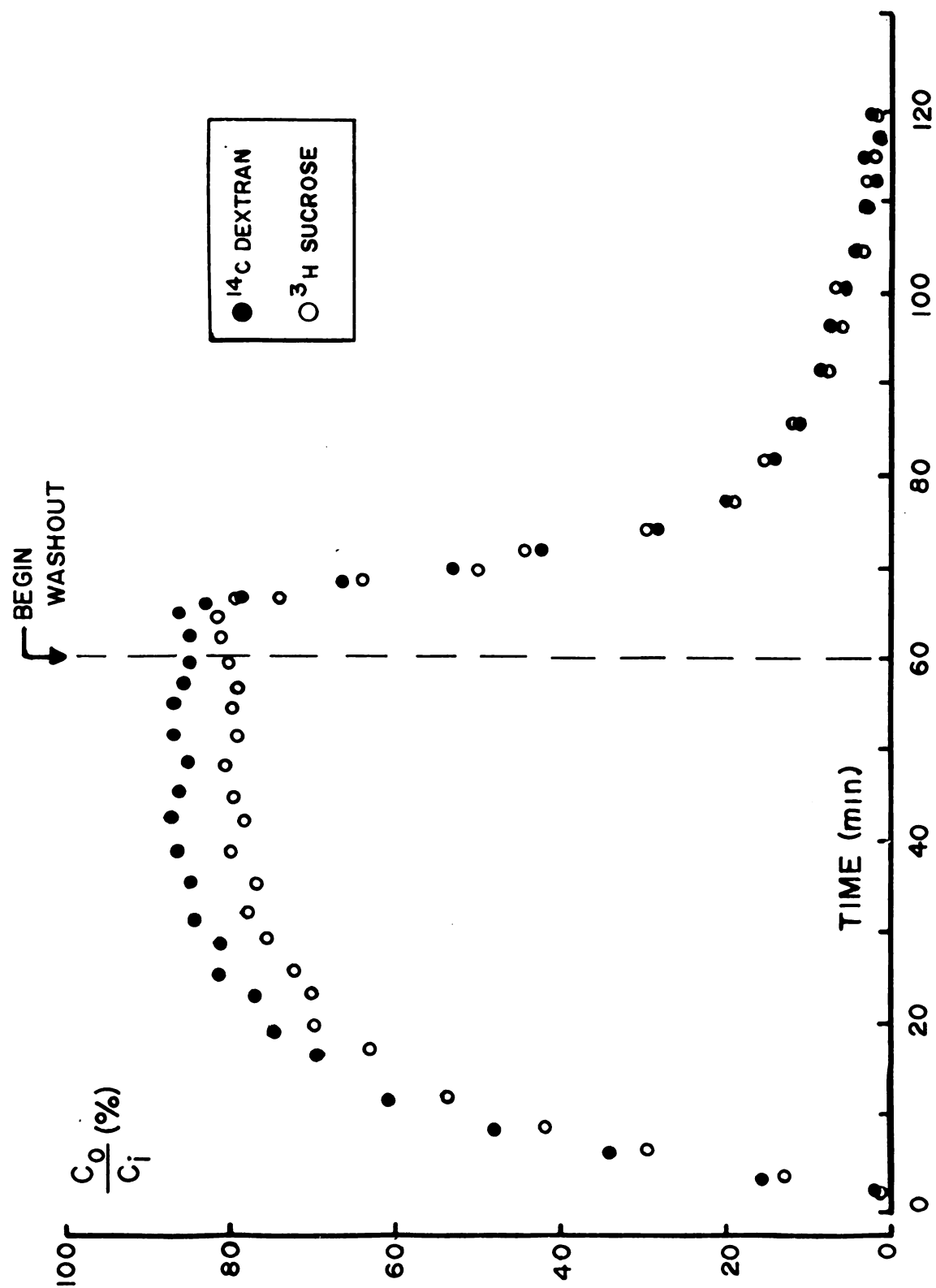
FIGURE 5

Table 5. Curve fitting analyses of the washout of sucrose and dextran during room air (A) and CO_2 (B) breathing.

Table 5A

| Cat # | ^{3}H-sucrose | | | | | ^{14}C-dextran | | | | |
	A	B	$-k_1$	$-k_2$	x^2 (x 10^{-3})	A	B	$-k_1$	$-k_2$	x^2 (x 10^{-3})
28	.838	.162	.483	.113	.21	–	–	–	–	–
DS 1	.926	.074	.374	.005	.13	.885	.115	.413	.083	.12
DS 4	.884	.116	.427	.063	.03	–	–	–	–	–
DS 5	.770	.230	.789	.084	.44	.823	.177	.611	.069	.39
DS 6	.926	.074	.572	.050	.10	.956	.044	.537	.050	.13
DS 7	.785	.215	.468	.078	.39	.839	.161	.386	.073	.44
Mean	.856	.145	.519	.074		.876	.124	.487	.069	
+SEM	.028	.028	.060	.009		.030	.030	.053	.007	

Table 5B

| Cat # | ^{3}H-sucrose | | | | | ^{14}C-dextran | | | | |
	A	B	$-k_1$	$-k_2$	x^2 (x 10^{-3})	A	B	$-k_1$	$-k_2$	x^2 (x 10^{-3})
30	.736	.264	.614	.059	.20	.832	.168	.305	.038	.48
DS 2	.903	.097	.391	.040	.09	–	–	–	–	–
DS 4	.931	.069	.326	.038	.08	–	–	–	–	–
DS 7	.839	.161	.496	.045	.11	.850	.150	.500	.055	.32
Mean	.852	.148	.457	.046						
+SEM	.043	.043	.063	.005						

The fit of the experimental washout data points to the general exponential equation: $Y(t) = Ae^{-k_1 t} + Be^{-k_2 t}$ is by a chi-square (x^2) minimization criterion (the least sum of squares between the predicted data point and the experimental data points) which were less than or equal to 0.0005.

VI. DISCUSSION

6.1. Effect of hypercapnia on arterial pH and PCO_2

Normal arterial blood pH values reported for awake, unrestrained cats vary in a range 7.37 to 7.43 and for PCO_2, 26.6 to 32.5 mm Hg (Fink et al., 1963; Herbert et al., 1971). These values are similar to those reported in the present study (Table 2 and Table G-1, Appendix G) for barbiturate anesthetized cats. The relatively low arterial PCO_2 (compared to man) is considered to be normal for the domestic cat (Fink et al., 1963) due to the smaller (40%) buffering capacity of the blood found in this species compared to that in man.

The elevation of P_aCO_2 induced by CO_2 inhalation (hypercapnia) has been well documented to cause vasodilation of the cerebral vasculature and an increase in brain blood flow (Reivich, 1964; Smith et al., 1971; Grubb et al., 1974). Brain blood flow (BBF) has been shown in mammals to vary linearly with P_aCO_2 over the range 15 to 70 mm Hg (Smith et al., 1971; Grubb et al., 1974), but it is not correlated with changes in arterial pH, other than those produced by changes in P_aCO_2 (Reivich, 1964). In the present study, it appears that BBF may be increased above air breathing levels since the P_aCO_2 values of hypercapnic cats (54 mm Hg) are at levels

which have been shown to induce increases in BBF.

6.2. Effect of hypercapnia on CSF formation

The technique of ventriculocisternal perfusion was used in this study to investigate the influence of an hypercapnic-induced increase in BBF on CSF phenomena since it permits the quantitative studies of CSF formation and absorption, the transport of substances among blood, brain and CSF, and an estimation of a CSF volume, simultaneously.

Inulin, a non-metabolizable molecule (M.W. = 5200) was used to estimate CSF formation since it has been shown that transependymal flux of inulin during perfusion of the brain ventricular system was negligible (Heisey et al., 1962; Rall et al., 1962). In the present study, mean CSF formation rate was 22.8 μl/min, a value similar to that previously reported for barbiturate anesthetized, air breathing cats (Snodgrass and Lorenzo, 1972; Weiss and Wertman, 1978), and it is similar to CSF formation values when inulin or albumin were used as the non-diffusible indicator (Table 1).

The formation of CSF has been shown to be altered by changes in body temperature (Snodgrass and Lorenzo, 1972), intracranial pressure (Hochwald and Sahar, 1971), systemic arterial blood pressure (Carey and Vela, 1974) and when P_aCO_2 is decreased below normocapnic levels by hyperventilation (Oppelt et al., 1963; Ames et al., 1965). However, the effect of raising P_aCO_2 by CO_2 inhalation on CSF formation in mammals has been the subject of several experimental studies

which have yielded inconsistent results. In this study, hypercapnia caused increases in CSF formation rates which are in agreement with data reported by Ames et al. (1965) who demonstrated an increased rate of CSF formation with an in situ preparation of the lateral ventricular choroid plexus in cats during 10% CO_2 inhalation. They indicated that this was due to the dilation of the choroidal blood vessels observed during hypercapnia.

Our results are contrary to data from investigators who used the ventriculocisternal perfusion technique as in this study to study the influence of hypercapnia on CSF production. They found that the rates of CSF formation were not altered by CO_2 breathing in various mammals (Oppelt et al., 1963 in dogs; Hochwald et al., 1973 in cats; Martins et al., 1976 in monkeys). The discrepancy between the results is explained on the basis of a cerebral perfusion pressure (CPP) criterion (Section 4.4., Methods) used in our study to account for the variations of both intracranial and systemic arterial pressures among experimental animals. Weiss and Wertman (1978) indicated that CSF formation rates were unaffected by alterations in either blood pressure or intracranial pressure as long as CPP was maintained above 70 mm Hg. They also found that CSF formation was dependent on blood pressure and intracranial pressure when CPP was lowered to 55 mm Hg or less. Using this as a criterion, we found animals in the present study which maintained a CPP greater than or equal to 68 mm Hg showed an increase in CSF formation

rates during hypercapnia (Table 3). This would indicate that the relative status of both intracranial and systemic arterial pressures must be considered in the estimation of CSF formation especially under conditions of hypercapnia where these parameters are more variable (Figure 3; Small et al., 1960).

Based upon the observation of Welch (1963) that about 25% of choroidal blood flow is secreted as CSF, the hypercapnia-induced increases in CSF formation are proposed to be due to an increase in BBF which influences the secretory activity of CSF producing sites (choroid plexus and/or extrachoroidal sites). However, a simple correlation does not exist between BBF and CSF formation since it has been shown that CSF formation decreased during hypoxia (Michael and Heisey, 1973), a period of increased BBF (Kety and Schmidt, 1948). These data suggest that CSF formation is performed by an oxidative metabolic system and that blood flow plays a secondary role in the formation of CSF.

6.3. Effect of hypercapnia on ventricular permeability

The permeability of the cerebral ventricles to lipid insoluble molecules varies inversely with molecular size (Heisey et al., 1962). It is presumed to be affected by changes in BBF (Heisey et al., 1970; Anderson and Heisey, 1975) and deterioration of the experimental preparation (Cserr, 1965; Anderson and Heisey, 1972). In the present study, the increase in K_{suc} (Table 3) may be explained by an

hypercapnia-induced increase in BBF since changes in K_{suc} were considered to be independent of time as indicated by reversing the animal's breathing sequences but still finding an increased K_{suc} (Table 3). Brain blood flow is hypothesized to cause a "sink" effect for some materials moving from CSF or brain into blood and increasing this sink function by hypercapnia may steepen the diffusion gradient and/or lessen the diffusion distance for material moving from CSF to brain tissue and to blood. In mammals, if the test materials are elevated significantly in the blood or infused simultaneously into CSF and blood, the sink function provided by BBF would be compromised. This would affect the concentration gradients of test molecules within the brain and indirectly affect the calculation of the molecular transfer coefficient (Section 4.6.4.; Equation 3, Methods) leading to more variability in CSF clearances.

6.4. Effect of hypercapnia on intracranial CSF volume

The initial response to inspiration of 8-10% CO_2 was a transient increase in the intraventricular pressure and a translocation of CSF perfusate ($\dot{V}_o$) through the low resistance cisternal needle (Figure 3). These data, which are similar to results reported by Hochwald et al. (1973) and Martins et al. (1976), indicate a hydraulic shift in intracranial fluid spaces during hypercapnia which reduced CSF volume. These competitive changes observed during hypercapnic induction and the subsequent displacement of CSF

volume through the cisternal needle have been related to an increase in brain vascular volume as a consequence of cerebral vasodilation within the confinement of a non-compliant dura mater and skull (Small et al., 1960; Smith et al., 1971). Wolff and Lennox (1930) observed an increase in pial vessel diameter with the induction of 5% CO_2 inhalation. Also, they measured a transient increase in intracranial pressure by a needle inserted in the cisterna magna which they interpreted was the result of an increased BVV as a consequence of pial vessel dilation induced by hypercapnia. From these data and the results of the present study, it is hypothesized that the reduction in CSF volume appears to occur predominantly in the subarachnoid space, the lining of which contains compliant veins and venous sinuses.

When CO_2 is removed as the inspired gas, a rapid decrease in BVV is speculated to occur. This would result in an accumulation of perfusion effluent within the brain case until a new perfusion outflow is attained as suggested by the evidence following hypercapnia withdrawal (Figure 3).

In the present study, the perfused CSF volumes were estimated in animals exposed to both air and CO_2 breathing (Section 4.6.5., Methods) which was to lend support to the hypothesis of a changing CSF volume following hypercapnia induction and withdrawal. Data reported in Table 4 show that the perfused volumes, from the lateral ventricle to cisterna magna of cats, were unaltered by hypercapnia, compared to those under air breathing conditions. These data are

interpreted to represent an unchanging ventricular CSF volume. Our perfusion volume for air breathing cats (approximately 600 µl) was found to be less than values previously reported for this species (750 µl, Cutler[b] et al., 1968; 740 µl, Sahar et al., 1970) indicating that our volume may be an estimate of the cerebral ventricles since it has been implicated that the estimation of distribution volumes included some portion of the cranial subarachnoid space (Cutler[b] et al., 1968; Sahar et al., 1971). These data suggest that with an unchanging ventricular volume, the displacement of CSF volume during hypercapnic induction is occurring distal to the cisterna magna, in the subarachnoid space.

Washout of test molecules from the perfused ventriculocisternal system were performed to demonstrate further that hypercapnia resulted in an unchanging ventricular CSF volume and a reduced subarachnoid space volume. A two compartment washout was indicated by the double exponential equations reported in Table 5. It is suggested that the initial exponential washout of test molecules is representing the clearance from the perfused volume, the cerebral ventricles. Based on the similarity of the initial rate constants of the washout equations under air and CO_2 breathing, it would suggest that ventricular CSF volume is unaffected by hypercapnia. This would support our distribution volume data (Table 4) of an unchanging cerebral ventricular volume during CO_2 breathing. The second

exponential which is slower than that representing the
ventricular washout is speculated to represent the molecular
clearance from a larger CSF volume, the subarachnoid space.
It is hypothesized that if the subarachnoid space were
reduced during hypercapnia, its exponential washout rate
would be slower than that during air breathing but our data
did not show this response. The lack of significance in
these data may be due to the subarachnoid space being an
unperfused compartment which behaved as a reservoir for fluid
that is not mixed with the inflow perfusate, thereby causing
a variable washout from this compartment.

Data presented in Figure 4 is interpreted to support
the hypothesis that there is an unmixed subarachnoid space
compartment. This is indicated by the transient reduction in
outflow concentration of test molecules when the animals
initially inspired CO_2. These reductions in effluent
concentrations occurred concurrently with the transient
increase in perfusion effluent ($\dot{V}_o$; Figure 3) and long after
steady state molecular concentrations were established in the
cisternal effluent. These data suggest that if the
subarachnoid space were reduced during hypercapnia, it would
contribute unmixed fluid to our effluent and reduce molecular
concentrations.

It is not clear whether a transient increase in CSF
formation occurred upon hypercapnia induction which caused
dilution of perfusion effluent concentrations (Figure 4) and
raised perfusion effluent ($\dot{V}_o$) transiently (Figure 3). This,

however, cannot be clearly differentiated from a reduction in CSF volume since an hypercapnia-induced increase in CSF formation occurred in our present study (Table 3), but it is a problem that warrants further investigations.

VII. SUMMARY

1. Brain ventricles of cats were perfused with an
    artificial CSF which yielded data on rates of CSF
    formation and absorption, molecular movement from the
    CSF, and the size of the cerebral ventricles.

2. Elevation of arterial carbon dioxide pressure (P_aCO_2) by
    8-10% CO_2 inhalation resulted in increases in the rates
    of CSF formation ($\dot{V}_f$) and molecular clearances from the
    brain ventricles (K_{suc}) in animals with cerebral
    perfusion pressure greater than or equal to 68 mm Hg.

3. Hypercapnic-induced increases in $\dot{V}_f$ and K_{suc} were
    independent of perfusion time suggesting that these were
    effects of an hypercapnia-induced increase in brain
    blood flow.

4. Hypercapnia induction produced transient increases in
    perfusion effluent rate ($\dot{V}_o$) and intraventricular
    pressure as well as a transient decrease in molecular
    outflow concentrations. These were interpreted to
    indicate a competitive reduction in CSF volume within
    the rigid brain case as a result of an increase in brain

68

vascular volume consequent to cerebral vasodilation. The brain ventricular volume of cats was approximately 600 μl and was not altered significantly by hypercapnia. It is suggested that the competitive shift of CSF volume was distal to the cisterna magna and from a volume that that was free of or which had a lower concentration of test molecules.

5.   Washout of test molecules from the ventriculocisternal system indicated a two compartment system which is speculated to be cerebral ventricles and subarachnoid space. The volumes of these compartments, as indicated by the rates of molecular removal during washout were not altered significantly by CO_2 breathing. The lack of significance in washout data to the hypothesis of a reduced CSF volume may be due to a nonmixing phenomenon in the subarachnoid space.

APPENDICES

pH and P_aCO_2 measurements

Reference: Radiometer instruction manual, Model PHA 927b, Radiometer A/S, Copenhagen, Denmark

Principle:

The pH electrode is designed to measure H^+ ion activity. The sample is drawn into a H^+-sensitive glass capillary which is surrounded by a buffer whose pH is approximately 6.40. The H^+ ion difference between the fluid sample and the sealed buffer generates a voltage potential which is measured by a calomel reference electrode and a Ag-AgCl glass electrode amplified and displayed on a scale calibrated in pH units (Model PHM27, The London Co., Cleveland, Ohio).

The CO_2 electrode (Model E5036, The London Co.) is a pH electrode in direct contact with a bicarbonate solution. The bicarbonate solution and electrode are separated from the sample being analyzed by a CO_2-permeable silicon rubber membrane which allows only gas molecules to pass through and not charged particles or ions. The CO_2 gas rapidly diffuses into the bicarbonate solution thus altering its pH. This altered pH generates a potential which is sensed by a galvanometer and the deflection is recorded on a scale calibrated in mm Hg PCO_2 (Model PHM27, The London Co.).

Calibration:

The CO_2 electrode is calibrated using two gases with known CO_2 composition (5% and 12% CO_2 with balanced N_2, 21% O_2, The London Co.). The pH electrode is standardized with commercial buffers at 38 $\pm$ 0.2°C (pH = 6.840 and pH = 7.383, Scientific Products Inc., Allen Park, MI).

Specimen:

Arterial blood is collected anaerobically via the femoral arterial cannula in a glass syringe, the dead space of which is filled with heparin (10,000 units/ml). The tip of the syringe is sealed with a metal cap filled with mercury. Mercury is introduced into the syringe to facilitate mixing of the blood specimen after collection and before analysis. Analyses of arterial pH and PCO_2 were performed in triplicate or until duplicate pH readings were $\pm$ 0.010 pH units and duplicate PCO_2 readings were $\pm$ 0.3 mm Hg. The thermostatted electrodes were adjusted approximately to rectal temperature (38 $\pm$ 0.5°C).

LIQUID SCINTILLATION COUNTING

Reference: Beckman Liquid Scintillation Counter manual,
Model 3150P, Beckman Instruments Inc., Fullerton, CA

Principle:

  Liquid scintillation counting is a method for the
detection of energy from an ionizing particle emitted by a
decaying nucleus. This energy is converted from kinetic
energy of an ionizing particle into light photons by a
solution of organic fluors and is detected by a
photomultiplier tube connected to amplifiers and a scalar
circuit. The decaying nucleus and the scintillation detector
(fluor) are in intimate contact, making the detection
efficiency quite high for use with low energy beta emitters
such as tritium and carbon-14.

Counting channel selection:

  The energy spectra of tritium and carbon-14 overlap
and when both beta emitters are present in the same sample,
they are counted simultaneously on 2 separate analyzer
channels. Channel 1 amplifiers are adjusted to give high
efficiency of counting tritium with minimal interference of
carbon-14; amplifiers of Channel 2 are set so that counting
efficiency of tritium is insignificant while efficiency for
carbon-14 is maximal. A separate amplifier is set to

maximize energy pulses from an external standard of known disintegration rate (137-cesium).

Quench correction curve:

Quenching is defined as any process which results in a decreased number or intensity of photons produced; this reduces the efficiency of counting the radioactivity. The amount of quench will be related to the probability of measuring the emissions from a sample; i.e., counting efficiency. To monitor the amount of quench in a sample and allow for corrections to give true sample activity, a method called external standard channel ratio (ESCR) is used. This measures the change in the ratio of pulses produced by an external gamma-ray source (137-cesium) between two selected counting channels as a function of the counting efficiency.

$$ESCR = \frac{T_2 - S_2}{T_1 - S_1} \qquad (B-1)$$

where:

T_1 or T_2 = counts per minute produced by the sample and external gamma source in channel 1 or 2.

S_1 or S_2 = counts per minute produced by the sample alone in channel 1 or 2.

The properly scaled number of events obtained in each channel during the sample count is subtracted from the events obtained during the total count (sample plus 137-Cs source) to give the net contribution from the gamma source observed in each channel. The ratio of the two net counts (2/1) is computed, and the resulting ESCR number is printed.

The quench correction curve (Figure B-1) is a plot of the efficiency of tritium and carbon-14 quench standards (Amersham/Searle, Boston, MA) as a function of the external standard channel ratio (ESCR). Counting efficiencies of each isotope in an unknown sample can be read directly from the quench correction curves (Figure B-1) corresponding to the unknown sample's external standard channel ratio (ESCR).

Tritium and carbon-14 detection

In these studies, dual-labelled counting procedures were used. ^{3}H-sucrose and ^{14}C-sucrose; or ^{3}H-sucrose and ^{14}C-dextran (New England Nuclear, Boston, MA) activities were measured both in the cisternal effluent and in the inflow perfusion fluid. The disintegration rates of unknown samples were calculated from the counts per minute of ^{3}H and ^{14}C and the selected efficiencies of counting each isotope in channels A or B.

Figure B-1. Quench standards correction curves for differential counting of ^{3}H and ^{14}C samples. Percent efficiencies of ^{3}H and ^{14}C quench standards (ordinate) were calculated as net counts per minute in channel A (set for ^{3}H photopeak) or channel B (set for ^{14}C above ^{3}H) divided by disintegrations per minute of tritium and carbon-14 quench standards. The abscissa is the external standard channel ratio (ESCR) as described and calculated by Equation B-1. Quench correction curve for ^{14}C efficiency in channel B (circles); quench correction curve for ^{3}H efficiency in channel A (squares); quench correction curve for ^{14}C efficiency in channel A (triangles).

Settings used on LS-3150P:

	Channel A	Channel B
Windows	tritium iso-set	carbon-14 iso-set
Gain	283	283
AQC/ESCR	.720	.720
Preset error	0.5%	0.5%
Preset time	20 min	20 min
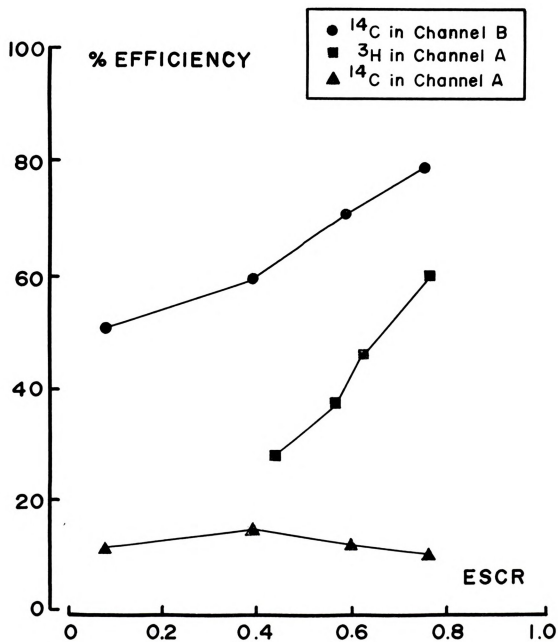
FIGURE B-1

Counting procedures and calculation of disintegration rates of ^3H and ^{14}C

The disintegration rates for ^3H and ^{14}C were calculated using a Hewlett-Packard programmable calculator (Model 67, Corvallis, Oregon) which was programmed for solving the following equations:

$$D_{3H} = \frac{N_1 c_2 - N_2 c_1}{h_1} \qquad (B-2)$$

$$D_{14C} = \frac{N_2}{c_2} \qquad (B-3)$$

where:

D_{3H} = disintegration rate (dpm) of tritium

D_{14C} = disintegration rate (dpm) of carbon-14

N_1 = net count rate in Channel A (cpm-bkgd cpm)

N_2 = net count rate in Channel B (cpm-bkgd cpm)

h_1 = counting efficiency for tritium in Channel A (%)

c_1 = counting efficiency for carbon-14 in Channel A (%)

c_2 = counting efficiency for carbon-14 in Channel B (%)

INULIN ASSAY

Direct Resorcinol Method without Alkali Treatment

Modified from H.W. Smith, 1956

Principle:

      A method in which inulin is hydrolyzed to fructose by heating in acid. Fructose molecules combine with resorcinol to yield a colored complex; the intensity of the color is proportional to the amount of fructose present.

Reagents:

    1. Resorcinol (Fisher Sci. Co., Fairlawn, New Jersey)

    2. Ethanol (95%)

    3. Hydrochloric acid (conc.)

Solutions:

    A. Resorcinol (1.0 mg/ml)

       Dissolve 200 mg resorcinol q.s. 200 ml with 95% ethanol. Prepare fresh daily.

    B. HCl (appoximately 8N)

       Add 224 ml of deionized water to 1000 ml conc. HCl.

Inulin standard solutions:

Dissolve 200 mg inulin (Pfanstiehl Laboratories, Inc., Waukegan, IL) in deionized water q.s. 100 ml (2.0 mg/ml). Dilute 7.5, 5.0, 4.0, 3.0, 2.0, and 1.0 ml of 2.0 mg/ml inulin solution to 10 ml with deionized water yielding 1.5, 1.0, 0.8, 0.6, 0.4, and 0.2 mg/ml inulin standards. Standards are stored at 4°C.

Procedure:

To duplicate 0.05 ml unknown samples, inulin standards and a CSF—reagent blank, 1.0 ml solution A and 2.5 ml solution B are added and mixed (vortex) in pyrex test tubes. A glass marble is placed on top of the tubes to prevent evaporation and tubes are incubated for 25 minutes at 80° C. Tubes are cooled in tap water for 3 minutes and optical density is determined within 1 hour at 410 nm (peak of absorbancy; Figure C-1) in plastic cuvettes (Scientific Products, Allen Park, MI) against a CSF—reagent blank in a Beckman DB spectrophotometer (Beckman Instruments, Inc., Fullerton, CA).

Figure C-1.   The optical density of a 1.0 mg/ml inulin solution (ordinate)
plotted as a function of wavelength (nm; abscissa). Two
absorbance peaks are observed at 410 nm and 470 nm wavelengths.
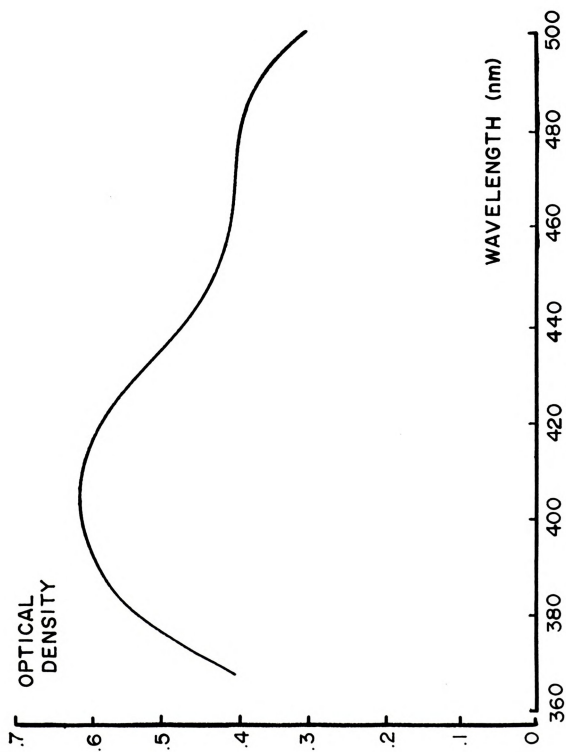
FIGURE C-1

Calculations:

Optical density at 410 nm plotted as a function of inulin concentration yields a straight line over the range 0-1.0 mg/ml inulin. Inulin concentration in unknown samples is calculated by multiplying the optical density of the unknown by the reciprocal of the slope of the standard curve (Figure C-2).

$$C_x = \left[\frac{C_s}{OD_s} \right]_a \times OD_x$$

where:

C = concentration

OD = optical density

s = standard

a = average

x = unknown sample

Figure C-2. The optical density of inulin standards
(ordinate) plotted as a function of known inulin
concentrations (mg/ml; abscissa).
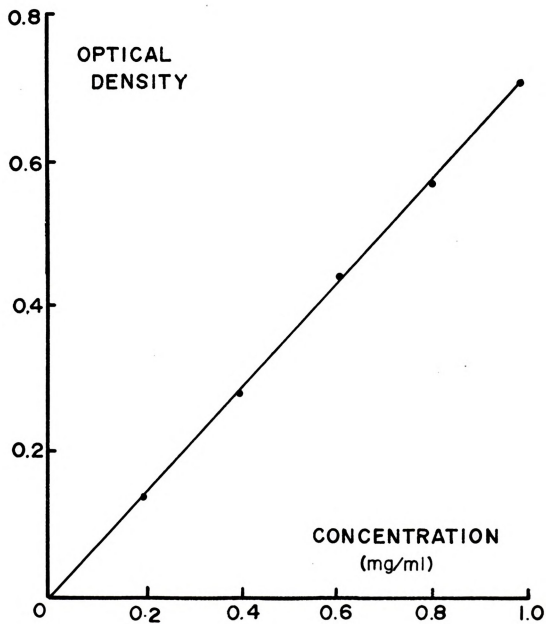
FIGURE C-2

Composition and Preparation of

Artificial Cat Cerebrospinal Fluid (CSF)

Cat CSF contains: Na, 130 mEq/l; K, 2.5 mEq/l; Cl, 132 mEq/l; HCO_3, 20 mEq/l; Ca, 2.5 mEq/l; Mg, 1.0 mEq/l (Vogh and Maren, 1975).

Reagents

    1. NaCl, Analytic reagent (A.R.)

    2. KCl, A.R.

    3. $NaH_2PO_4 \cdot H_2O$, A.R.

    4. $Na_2HPO_4 \cdot 7H_2O$, A.R.

    5. $NaHCO_3$, A.R.

    6. $MgSO_4 \cdot 7H_2O$, A.R.

    7. $CaCl_2$, A.R.

Solutions

    A. 7.6 g of reagent 1; 186.4 mg of reagent 2; 169.0 mg of reagent 3; 134.0 mg of reagent 4; 1.68 g of reagent 5 are dissolved in deionized water; q.s. to one liter.

    B. 24.65 g of reagent 6 is dissolved in deionized water; q.s. to 100 ml.

    C. 27.75 g of reagent 7 is dissolved in deionized water; q.s. to 100 ml.

Procedure

The pH of solutions A is adjusted to approximately 7.40 by bubbling with 5% CO_2 at room temperature for 30 minutes. Then 0.1 ml of solutions B and C are added to 100 ml of solution A to give the normal ionic concentrations of cat CSF.

APPENDIX E

Dial-Urethane solution

Reagents

      1.   Diallyl barbituric acid (crystalline; K&K Laboratories, Inc., Plainview, NY).

      2.   Monoethyl urea (Pfaltz and Bauer, Inc., Flushing, NY).

      3.   Urethane (Aldrich Chemical Co., Milwalkee, WI).

      4.   Disodium calcium ethylene diamine tetra acetate trihydrate (Pfaltz and Bauer, Inc., Flushing, NY)

Procedure

Dissolve 10.0 g urethane, 40.0 g monoethyl urea, 50.0 mg disodium calcium ethylene diamine tetra acetate trihydrate, and 40.0 g diallyl barbituric acid in 10 ml of deionized water. Heat in a water bath to dissolve chemicals. Cool to room temperature and store in stoppered dark glass bottle at room temperature.

APPENDIX F

Method of Non-Linear Least Squares

Reference: Bevington, P.R. (1969)

Principle

The method of non-linear least squares is a technique
for fitting experimental data points (x_i, y_i) with a function
y(x) which is not linear with respect to its parameters such
as:

$$Y(x) = Ae^x \qquad\qquad (F-1)$$

where:

A = coefficient (parameter)

e^x = exponential rise for any given value of x
(parameter)

The application is to fit straight lines to a set of
experimentally observed points for any dependent variable, y,
and for any independent variable, x. For a straight line
which comes close to fitting most of the observed data
points, some of the deviations will be positive and some will
be negative (random scatter of data points along the straight
line). By squaring the deviations and requiring that the sum
of squares of the deviations be minimized, the expression

counts a positive deviation and a negative deviation equally. The curve fitted to these experimentally observed points is considered to be of best fit when it produces the smallest sum of squares of the deviations or a "least-squares fit".

The criterion for minimizing the parameters of a given equation is such that the discrepancy between the values of the measured y_i and the corresponding predicted values $y = f(x_i)$ are relatively small and can be found utilizing a chi-square test.

$$x^2 = \sum_{j=1}^{n} \left[Y_{tj} - Y_{dj} \right]^2 \qquad (F-2)$$

where:

x^2 = chi-square, a statistical measure of the dispersion of the observed (actual) distribution versus the theoretical (predicted) distribution.

Y_{tj} = theoretical jth data point (predicted)

Y_{dj} = experimental jth data point (actual)

n = total number of data points

The minimized value of the chi-square function is one which yields a value near zero (less than or equal to 0.0005) when the predicted fit of the curve is a close approximate of the experimentally observed curve.

Procedure

The washout of CSF-containing spaces (Figure 5; 60-120 minutes; Results) from perfusion of the ventriculocisternal system were interactively and systematically analyzed by a mini-computer (PDP-11, Digital Equipment Corp., Maynard, MA) using the method of non-linear least squares (Figure F-1). The chi-square function (Equation F-2) is the best fit criterion for fitting non-linear equations to experimentally determined points. A double exponential equation which best fit the transient washout data obtained from the perfusion experiments is:

$$Y(t) = Ae^{-k_1 t} + Be^{-k_2 t} \qquad \text{(F-3)}$$

where:

$Y(t)$ = molecular concentration in the CSF ventricular system at any time (t)

t = time (minutes)

A,B = are coefficients (parameters) of an exponential function. When $t=0$; $Y(0) = A + B$ = mean steady-state concentration.

When $t=\infty$; $Y(\infty) = 0$, the washout of CSF brain fluid spaces is complete.

k_1,k_2 = are rate constants (parameters) of the exponential function.

Figure F-1. Flow chart of algorithm (Bevington, 1969) used
to find the best non-linear numerical equation
to fit the experimental washout data to a double
exponential equation: $Y(t) = Ae^{-k_1 t} + Be^{-k_2 t}$
(Equation F-3). Best fit is determined by
finding iterative values of A, B, k_1, k_2 by a
chi-square minimization test computed from a
non-linear least squares method.
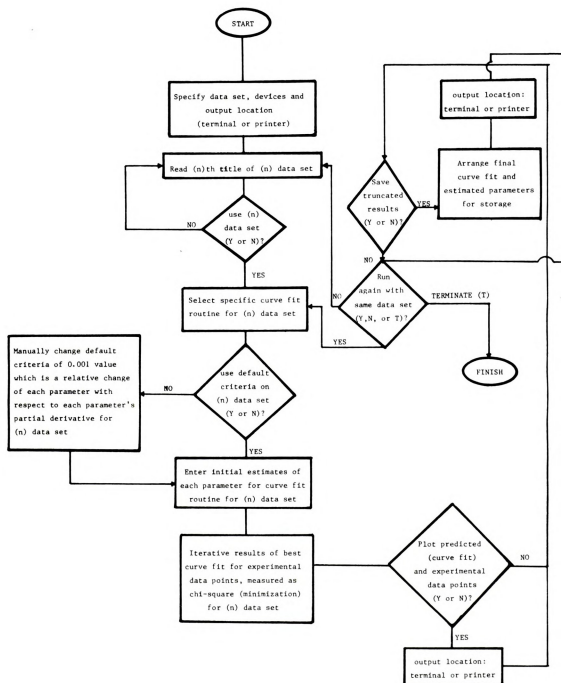
FIGURE F-1

The application of the exponential washout equation can be extended towards predicting the relative time when perfusion of the ventriculocisternal system began (time zero) without having to include cannulae dead space volume. The dead space volume is represented by a time delay occuring between the time when CSF containing test molecules is begun and the time when a measurable concentration is detected in the cisternal effluent (Figure 5; 0-2 minutes)

The curve fitting program generates a time zero (predicted) from the experimentally determined washout data. The predicted time zero is then subtracted from the actual time when CSF free of test molecules was first introduced through the ventricular needles (Figure F-2). This difference is the time lag that is presumably due to cannulae dead space volume. The value for the time lag can then be subtracted from the initial time when CSF containing test molecules was first introduced through the ventricular needles. This will result in an adjusted perfusion time zero from which to calculate a distribution volume of the ventriculocisternal system (Section 4.6.5., Methods).

Figure F-2.   Data in this figure show outflow concentration of sucrose (C_o/C_i; ordinate) as a function of time (min; abscissa) during washout with artificial CSF free of sucrose in an animal breathing CO_2 (Cat# DS4). Previous to time zero (not shown) a steady state concentration of sucrose was established in the perfusion system. At zero time, the inflow fluid containing no sucrose was introduced through the ventricular needles which resulted in an unchanging effluent sucrose concentration initially (time lag) due to dead space of perfusion cannulae. The intersection of the optimized steady state concentration (Methods; Section 4.7.1.) with the predicted washout curve (time = 4 min) predicts a new perfusion time zero.
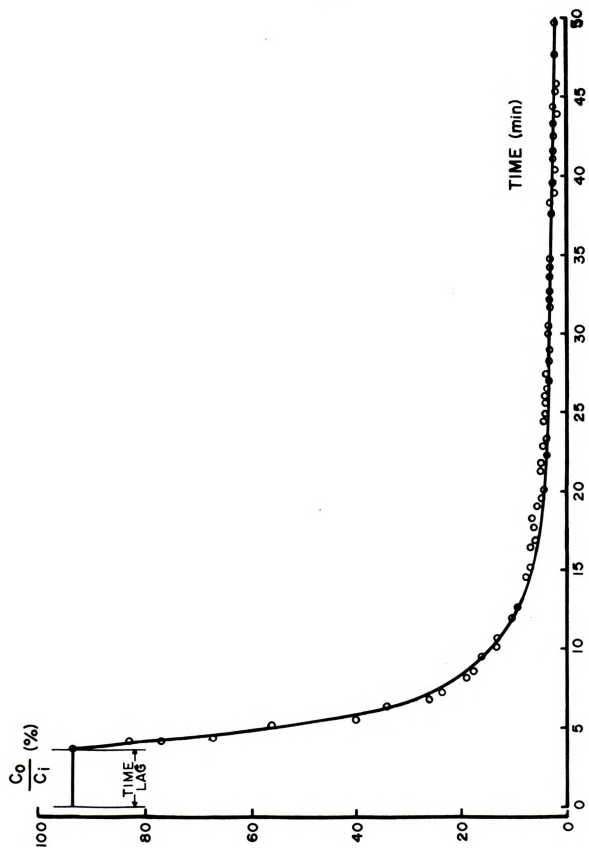
FIGURE F-2

MEASURED AND CALCULATED STEADY STATE DATA

Data in Table G-1 are measured steady state
quantities from 9 cats breathing room air and 8-10% CO_2 in
room air mixture during ventriculocisternal perfusion which
allowed calculation of CSF perfusion phenomena (Table G-2).

Definition of symbols:

$\dot{V}_i$ = perfusion inflow rate

$\dot{V}_o$ = perfusion outflow rate

$\dot{V}_f$ = CSF formation rate

$\dot{V}_a$ = CSF bulk absorption rate

C_o/C_i = molecular outflow concentration expressed as a
ratio of perfusion inflow concentration.

S^2 = variances of steady state molecular outflow
concentration ($x\ 10^{-3}$).

I,S = inulin and sucrose

pH = (logarithmic) hydrogen ion concentration

P_aCO_2 = arterial partial pressure of carbon dioxide

$CSFP$ = intraventricular pressure

$MABP$ = mean arterial blood pressure

K_{suc} = outflux rate of sucrose from cerebral ventricles

Table G-1 and Table G-2 show data from experiments which satisfied two experimental criteria: (1) in the steady state the total fluid volume input ($\dot{V}_i + \dot{V}_f$) was equal to the total fluid volume output ($\dot{V}_o + \dot{V}_a$) during ventriculocisternal perfusion and (2) the variances (S^2) of inulin and sucrose concentrations were equal to or less than 0.0010.

Table G-1. Measured parameters

| | ROOM AIR | | | | | | | | | | 8-10% CO_2 | | | | | | | | | |
CAT#	$\dot{V}_1$ (μl/min)	$\dot{V}_o$	C_o/C_1 I	C_o/C_1 S	S^2* I	S^2* S	pH_a	P_aCO_2 (mm Hg)	CSFP (cm H_2O)	MABP (mm Hg)	$\dot{V}_1$ (μl/min)	$\dot{V}_o$	C_o/C_1 I	C_o/C_1 S	S^2* I	S^2* S	pH_a	P_aCO_2 (mm Hg)	CSFP (cm H_2O)	MABP (mm Hg)
8	144	158	.83	.78	.3	.3	-	-	5	107	146	194	.85	.58	.7	.3	-	-	8	108
10	144	152	.86	-	.2	-	7.48	24	3	68	144	166	-	.64	-	-	-	-	3	72
12	144	155	.91	.86	.7	.7	7.35	30	6	92	144	187	.78	.74	.5	.5	7.12	52	8	87
13	145	154	.88	.85	.7	.1	7.30	36	7	97	145	174	.79	-	.5	.2	7.13	64	7	87
14	143	163	.77	-	.7	-	7.30	36	7	97	-	-	-	-	-	-	-	-	-	-
15	143	169	.83	-	.8	-	7.35	35	5	103	-	-	-	-	-	-	-	-	-	-
17	144	150	.97	.87	.2	.7	7.38	31	6	80	144	155	.90	.82	.5	.8	7.16	56	4	123
18	143	160	.84	.79	.1	.7	7.36	35	9	57	-	-	-	-	-	-	-	-	-	-
20	144	141	-	.77	-	.4	7.35	36	9	73	144	150	.90	.90	.3	.2	7.22	65	6	93
21	140	162	.82	.77	.5	.4	7.39	35	3	122	142	167	.78	.78	.9	.9	7.22	50	7	135
22	139	143	.87	.81	.4	.4	7.37	24	6	72	140	146	.81	.71	.6	1.0	7.08	51	5	108
23	140	149	.90	.83	.1	.1	7.36	21	3	58	140	152	.91	.82	.6	.2	7.10	53	1.5	89
24	159	154	.90	.88	.4	.5	7.26	29	4	130	-	-	-	-	-	-	-	-	-	-
25	139	147	.89	.88	.5	.9	-	-	4	58	-	-	-	-	-	-	-	-	-	-
26	140	156	.84	.80	.2	.3	-	-	9	75	-	-	-	-	-	-	-	-	-	-
28	140	151	.86	.78	.8	.4	-	-	4	52	-	-	-	-	-	-	-	-	-	-
30	-	-	-	-	-	-	-	-	-	-	139	147	.83	.81	.2	.3	7.12	59	7	65
DS4	139	122	.90	.81	.4	.2	7.26	27	5	97	139	119	.94	.92	.2	.1	6.95	-	4	80
DS6	144	146	-	.79	.1	.1	7.26	27	7.5	97	144	146	.94	.89	.1	.3	6.95	50	7.5	80

* (x 10^{-3})

Table G-2. Calculated parameters

ROOM AIR   8-10% CO_2

CAT#	$\dot{V}_f$ (μl/min)	$\dot{V}_a$ (μl/min)	K_{suc} (μl/min)	Absorption Resistance (cm H_2O/μl-min^{-1})	CPP (mm Hg)	$\dot{V}_f$ (μl/min)	$\dot{V}_a$ (μl/min)	K_{suc} (μl/min)	Absorption Resistance (cm H_2O/μl-min^{-1})	CPP (mm Hg)
8	30.5	16.5	9.2	0.3	104	48.0	0	44.3	u	101
10	27.7	14.7	-	0.2	65	-	-	-	-	-
12	14.2	3.2	7.8	1.6	88	39.9	0	29.3	u	81
13	20.5	11.5	5.0	0.6	92	39.5	10.5	9.0	0.7	82
14	42.7	22.7	-	0.3	92	-	-	-	-	-
15	29.5	3.5	-	1.4	99	-	-	-	-	-
17	4.6	0	14.8	u	76	16.2	5.2	14.7	0.8	120
18	27.2	10.2	9.6	0.9	50	-	-	-	-	-
20	-	-	-	-	-	16.2	10.2	0	0.6	89
21	31.8	9.8	9.8	0.3	101	-	-	-	-	-
22	20.2	16.2	1.5	0.4	68	33.5	27.5	19.7	0.2	104
23	15.9	23.5	12.5	0.4	45	13.2	1.2	16.0	1.3	85
24	18.5	9.2	2.5	0.2	127	-	-	-	-	-
25	17.2	9.2	1.7	0.4	55	-	-	-	-	-
26	26.7	10.7	7.6	0.8	68	-	-	-	-	-
28	22.8	11.8	14.5	0.3	49	-	-	-	-	-
30	-	-	-	-	-	29.3	21.3	3.2	0.3	60
DS4	14.9	31.9	16.4	0.2	86	8.4	28.4	14.2	0.2	64
DS6	-	-	-	-	-	9.5	7.5	8.3	1.0	37
MEAN	22.8	12.6	8.7	0.55		25.4	11.2	15.9	0.64	
±SEM	2.3	2.1	1.4	0.11		4.5	3.4	4.1	0.14	
n=	16	16	13	15		10	10	10	8	

u = undefined

BIBLIOGRAPHY

BIBLIOGRAPHY

Anderson, D. K. and S. R. Heisey. Clearance of molecules from cerebrospinal fluid in chickens. Am. J. Physiol. 222:645-648, 1972.

Anderson, D. K. and S. R. Heisey. Creatinine, potassium, and calcium flux from chicken cerebrospinal fluid. Am. J. Physiol. 229:415-419, 1975.

Ames, A., K. Higashi, and F. Nesbitt. Effects of PCO_2, acetazolamide and ouabain on volume and composition of choroid-plexus fluid. J. Physiol. 181:516-524, 1965.

Bering, E. A.. Composition of cerebrospinal fluid under varying conditions. Neurology 8:129-130, 1958.

Bering, E. A.. Cerebrospinal fluid production and its relationship to cerebral metabolism and cerebral blood flow. Am. J. Physiol. 197:825-828, 1959.

Bering, E. A. and O. Sato. Hydrocephalus: changes in formation and absorption of cerebrospinal fluid within the cerebral ventricles. J. Neurosurg. 20:1050-1063, 1963.

Brierly, J. B. Penetration of P^{32} into the nervous tissues of the rabbit. J. Physiol. 116:24P, 1952.

Calhoun, M. C., H. D. Hurt, and H. D. Eaton. Rates of formation and absorption of cerebrospinal fluid in Holstein male calves. Bull Univ Conn Agric. Exper. Sts. 401:22-36, 1967.

Carey, M. E. and A. R. Vela. Effect of systemic arterial hypotension on the rate of CSF formation in dogs. J. Neurosurg. 41:350-355, 1974.

Clemedson, C. J., H. Hartelius and G. Holmberg. The influence of carbon dioxide inhalation on the cerebral vascular permeability to trypan blue ('The Blood-Brain Barrier'). Acta Pathol. Microbiol. Scand. 42:137-145, 1958.

Cserr, H.. Physiology of the choroid plexus. Physiol. Rev. 51:273-311, 1971.

Cserr, H. Potassium exchange between cerebrospinal fluid, plasma, and brain. Am. J. Physiol. 209:1219-1226, 1965.

Curl, F.D. and M. Pollay. Transport of water and electrolytes between brain and ventricular fluid in the rabbit. Exp. Neurol. 20:558-574, 1968.

Cutler, R. W. P. and C. F. Barlow. The effect of hypercapnia on brain permeability to protein. Arch. Neurol. 14:54-63, 1966.

Cutler[a], R. W. P., L. Page, J. Galicich, and G.V. Watters. Formation and absorption of cerebrospinal fluid in man. Brain 91:707-720, 1968.

Cutler[b], R. W. P., R. J. Robinson, and A. V. Lorenzo. Cerebrospinal fluid transport of sulfate in the cat. Am. J. Physiol. 214:448-454, 1968.

Cutler[c], R. W. P. and A. V. Lorenzo. Transport of 1-aminocyclopentane carboxylic acid from feline cerebrospinal fluid. Science 161:1363-1364, 1968.

Dandy, W. E. and K. D. Blackfan. Internal hydrocephalus. An experimental clinical and pathological study. Amer. J. Dis. Child. 8:406-482, 1914.

Dandy, W. E. Experimental hydrocephalus. Ann. Surg. 70:129-142, 1919.

Davson, H., C. R. Kleeman, and E. Levin. Quantitative studies of the passage of different substances out of the cerebrospinal fluid. J. Physiol. 161:126-142, 1962.

Davson, H. Physiology of the Cerebrospinal Fluid. J. and A. Churchill Ltd., London, 1967.

Davson, H., G. Hollington, and M. B. Segal. The mechanism of drainage of the cerebrospinal fluid. Brain 93:665-678, 1970.

Fink, B. R., M. Schoolman. Arterial blood acid-base balance in unrestrained waking cats. Proc. Soc. Exp. Biol. Med. 112:328-330, 1963.

Flexner, L. B. and H. Winters. The rate of formation of cerebrospinal fluid in etherized cats. Am. J. Physiol. 101:697-710, 1932.

Fog, M.   Reaction of pial arteries to epinephrine by direct application and by intravenous injection.   Arch. Neurol. Psychiat. 41:109-118, 1939.

Frazier, C. H. and M. M. Peet.   Factors of influence of in the origin and circulation of the cerebrospinal fluid.   Am. J. Physiol. 35:268-282, 1914.

Goldberg, M. A., C. F. Barlow, and L. J. Roth.   Abnormal brain permeability in CO_2 narcosis. Arch. Neurol. 9:498-507, 1963.

Gottfried, B. S. and J. Weisman.   Introduction to Optimization Theory.   Prentice-Hall International New York, 1973.

Graziani, L., A. Escriva, and R. Katzman.   Exchange of calcium between blood, brain, and cerebrospinal fluid. Am. J. Physiol. 208:1058-1064, 1965.

Grubb, R. L., M. E. Raichle, and J. O. Eichling.   The effects of changes in P_aCO_2 on cerebral blood volume, blood flow, and vascular mean transit time.   Stroke 5:630-639, 1974.

Heisey, S. R., D. Held, and J. R. Pappenheimer.   Bulk flow and diffusion in the cerebrospinal fluid system of the goat.   Am. J. Physiol. 203:775-781, 1962.

Heisey, S. R.   Cerebrospinal and extracellular fluid spaces in turtle brain.   Am. J. Physiol. 291:1564-1567, 1970.

Heisey, R. R. and D. K. Michael.   Cerebrospinal fluid formation and bulk absorption in the freshwater turtle. Exp. Neurol. 31:258-262, 1971.

Herbert, D. A. and R. A. Mitchell.   Blood gas tensions and acid-base balance in awake cats.   J. Appl. Physiol. 30:434-436, 1971.

Hochwald, G. M. and M. Wallenstein.   Exchange of albumin between blood, cerebrospinal fluid and brain in the cat.   Am. J. Physiol. 212:1199-1204, 1967.

Hochwald, G. M. and A. Sahar.   Effect of spinal fluid pressure on cerebrospinal fluid formation.   Exp. Neurol. 32:30-40, 1971.

Hochwald, G. M., C. Malhan and J. Brown.   Effect of hypercapnia on CSF turnover and blood-CSF barrier to protein.   Arch. Neurol. 28:150-155, 1973.
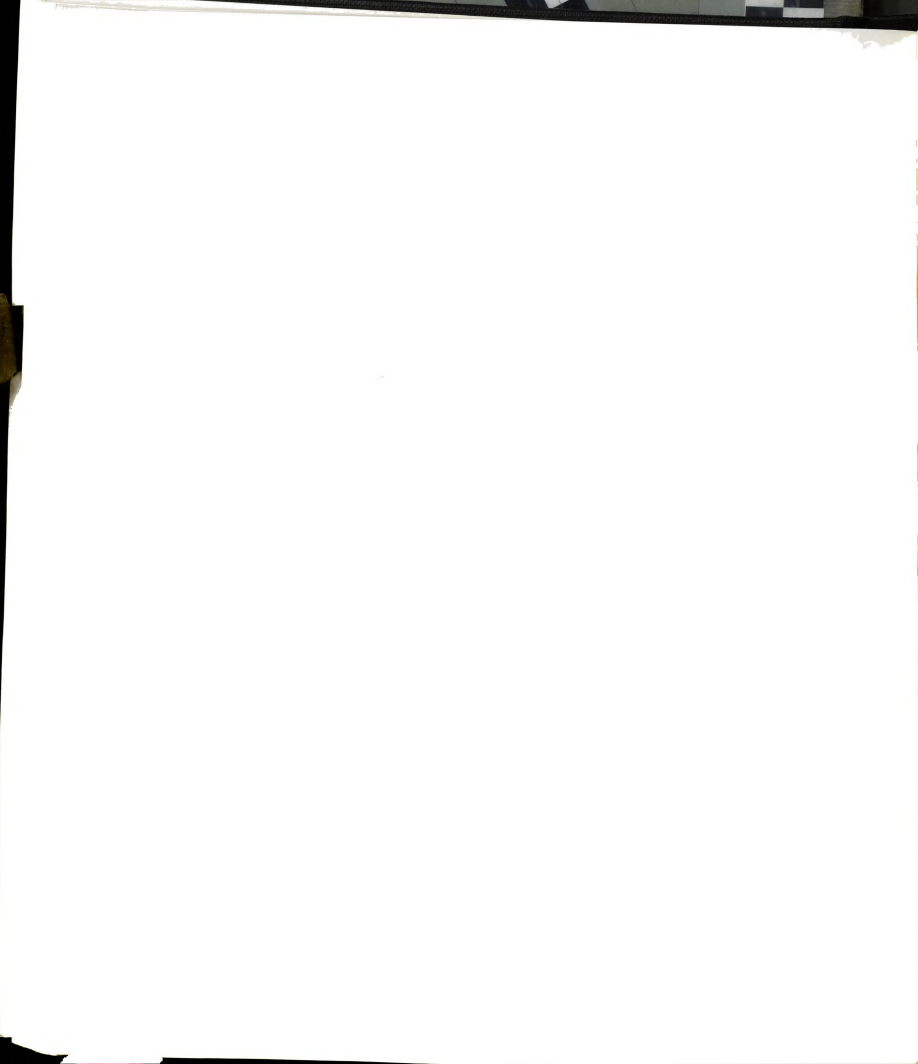
Katzman, R., L. Graziani, R. Kaplan, and A. Escriva. Exchange of cerebrospinal fluid potassium with blood and brain. Arch. Neurol. 13:513-524, 1965.

Kety, S. S. and C. F. Schmidt. The effects of altered arterial tension of carbon dioxide and oxygen on cerebral blood flow and cerebral oxygen consumption of normal young men. J. Clin. Invest. 27:484-492, 1948.

Lending, M., L. B. Slobody, and J. Mestern. Effect of hyperoxia, hypercapnia and hypoxia on blood-CSF barrier. Am. J. Physiol. 200:959-963, 1961.

Macri, F. J., A. Politoff, R. Rubin, R. Dixon, and D. Rall. Preferential vasoconstriction properties of acetazolamide on the arteries of the choroid plexus. Int. J. Neuropharmacol. 5:109-115, 1966.

Maren, T. H. Carbonic anhydrase: chemistry, physiology and inhibition. Physiol. Rev. 47:595-781, 1967.

Martins, A., T. Doyle, and N. Newby. PCO_2 and rate of formation of cerebrospinal fluid in monkey. Am. J. Physiol. 231:127-131, 1976.

Martins, A. N., N. Newby, and T. F. Doyle. Sources of error in measuring cerebrospinal fluid formation by ventriculocisternal perfusion. J. Neurol. Neurosurg. and Pyschiat. 40:645-650, 1977.

Michael, D. K. and S. R. Heisey. Effects of brain ventricular perfusion and hypoxia on CSF formation and absorption. Exp. Neurol. 41:769-772, 1973.

Milhorat, T. H. Choroid plexus and cerebrospinal fluid production. Science 166:1514-1516, 1969.

Milhorat, T. H., M. K. Hammock, J. D. Fernstermacher, D. P. Rall, and V. A. Levin. Cerebrospinal fluid production by the choroid plexus and brain. Science 173:330-332, 1971.

Oppelt, W. W., T. Maren, E. S. Owens, and D. P. Rall. Effects of acid-base alterations on cerebrospinal fluid formation. Proc. Soc. Exp. Biol. Med. 114:86-89, 1963.

Pollay, M. and K. Welch. The function and structure of canine arachnoid villi. J. surg. Res. 2:307-311, 1962.

Pollay, M. and H. Davson. The passage of certain substances out of the cerebrospinal fluid. Brain 86:137-150, 1963.

Pollay, M. and F. Curl. Secretion of cerebrospinal fluid by the ventricular ependyma of the rabbit. Am. J. Physiol. 213:1031-1038, 1967.

Pollay, M. Formation of cerebrospinal fluid. J. Neurosurg. 42:665-673, 1975.

Pappenheimer, J. R., S. R. Heisey, and E. F. Jordan. Active transport of Diodrast and phenolsulfonphthalein from cerebrospinal fluid to blood. Am. J. Physiol. 200:1-10, 1961.

Pappenheimer, J. R., S. R. Heisey, E. F. Jordan, and J. de C. Downer. Perfusion of the cerebral ventricular system in unanesthetized goats. Am. J. Physiol. 203:763-774, 1962.

Rall, D. P., W. W. Oppelt, and C. S. Patlak. Extracellular space of brain as determined by diffusion of inulin from the ventricular system. Life Sciences. 2:43-48, 1962.

Reivich, M.. Arterial PCO_2 and cerebral hemodynamics. Am. J. Physiol. 206:25-35, 1964.

Riggs, D. S. The Mathematical Approach to Physiological Problems. "A Critical Primer". The MIT press, Massachusetts, 1963.

Rosomoff, H. L. and D. A. Holaday. Cerebral blood flow and cerebral oxygen consumption during hypothermia. Am. J. Physiol. 179:85-88, 1954.

de Rougemont, J., A. Ames III, F. B. Nesbitt, and H. F. Hofmann. Fluid formed by choroid plexus. A technique for its collection and a comparison of its electrolyte composition with serum and cisternal fluids. J. Neurophysiol. 23:485-495, 1960.

Sahar, A., G. M. Hochwald, and J. Ransohoff. Experimental hydrocephalus: cerebrospinal fluid formation and ventricular size as a function of intraventricular pressure. J. Neurol. Sci. 11:81-91, 1970.

Schreiner, G. E. Determination of inulin by means of resorcinol. Proc. Soc. Exp. Med. 74:117-120, 1950.

Shipley, R. A. and R. E. Clark. Tracer Methods for in vivo Kinetics. Academic Press., New York, 1972.

Small, H. S., S. W. Weitzner and G. G. Nahas. Cerebrospinal fluid pressures during hypercapnia and hypoxia in dogs. Am. J. Physiol. 198:704-708, 1960.

Smith, A. L., G. R. Neufeld, A. J. Ominsky, and H. Wollman. Effect of arterial CO_2 tension on cerebral blood flow, mean transit time, and vascular volume. J. Appl. Physiol. 31:701-707, 1971.

Smith, H. W.. Principles of Renal Physiology. Oxford University Press, New York, 1956.

Snodgrass, S. R. and A. V. Lorenzo. Temperature and cerebrospinal fluid production rate. Am. J. Physiol. 222:1524-1527, 1972.

Sokal, R. R. and F. J. Rohlf. Introduction to Biostatistic. W. H. Freeman and Company, San Fransisco, 1969.

Tschirgi, R. D. Protein complexes and the impermeability of the blood-brain barrier to dyes. Am. J. Physiol. 163:756P, 1950.

Vogh, B. P. and T. H. Maren. Sodium and chloride, bicarbonate movement from plasma to cerebrospinal fluid in cats. Am. J. Physiol. 228673-683, 1975.

Weed, L. H. The pathways of escape from the subarachnoid spaces with particular reference to the arachnoid villi. J. Med. Res. 31:51-91, 1914.

Weed, L. H. and L. B. Flexner. The relations of the intracranial pressures. Am. J. Physiol. 105:266-272,1933.

Weiss, M. H. and N. Wertman. Modulation of cerebrospinal fluid production by alteration in cerebral perfusion pressures. Arch. Neurol. 35:527-529,1978.

Welch, L. and V. Friedman. The cerebrospinal fluid valves. Brain 83:454-469, 1960.

Welch, K and M. Pollay. Perfusion of particles through arachnoid villi of the monkey. Am. J. Physiol. 201:651-654, 1961.

Welch, K.. Secretion of cerebrospinal fluid by the choroid plexus of the rabbit. Am. J. Physiol. 205:617-624, 1963.

White, J. C., M. Verlot, B. Selverstone,and H. K. Beecher. Changes in brain volume during anesthesia: The effects of anoxia and hypercapnia. Arch Surg. 44:1-21, 1942.

Wolff, H. G. and H. S. Forbes. Observations of the pial circulation during changes in intracranial pressure. Arch Neurol. Psychiat. 20:1035-1047, 1928.

Wolff, H. G. and W. G. Lennox. The effect on the pial vessels
    of variations in the oxygen and carbon dioxide content
    of the blood. Arch. Neurol. Psychiat. 23:1097-1120,
    1930.